Molecular dynamics simulations of membranes

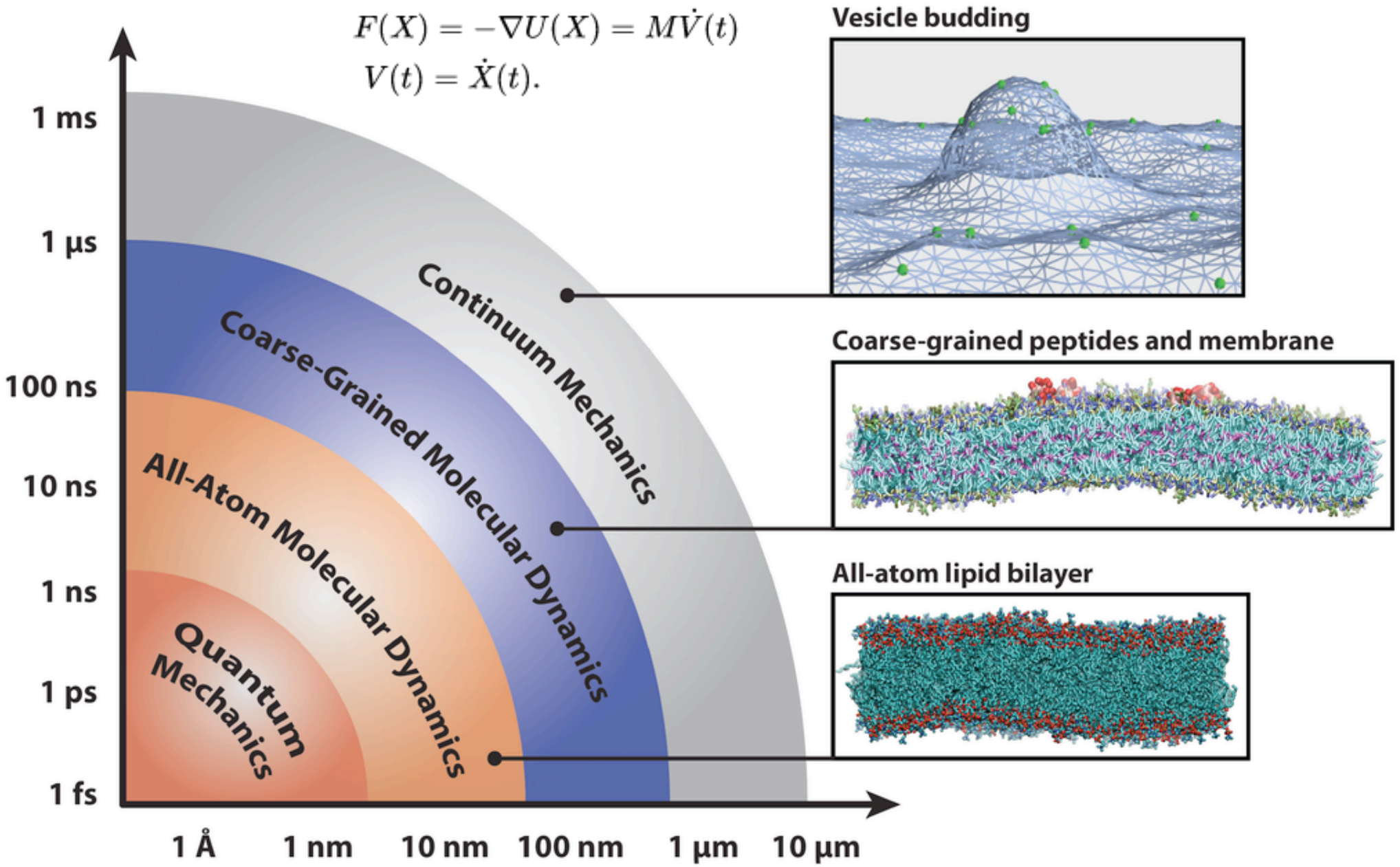

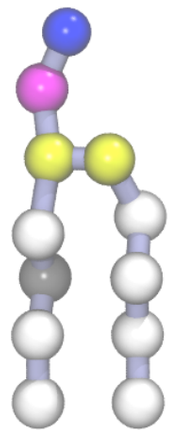

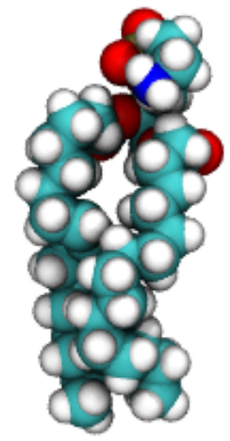

Figure 1. Diagram of computational methods for studying biophysical systems across a range of time- and length-scales. Representative snapshots depict an all-atom lipid bilayer, peptides embedded in a coarse-grained bilayer and proteins remodeling a continuum mechanics membrane model. Bilayers were simulated with the CHARMM36 [15] and Martini [16] force fields and rendered with Visual Molecular Dynamics [17].

Bradley & Rhadakrishnan, *Polymers* **2013**, *5*(3), 890-936; https://doi.org/10.3390/polym5030890

Molecular dynamics simulations of membranes

<u>Simulation details</u>
Software: Gromacs
FF: MARTINI
Simulation time: 160 μs total
10 + 8 replicas

<u>Lipid composition</u>
headgroup: 67% PE, 33% PG
tails: 100% PO

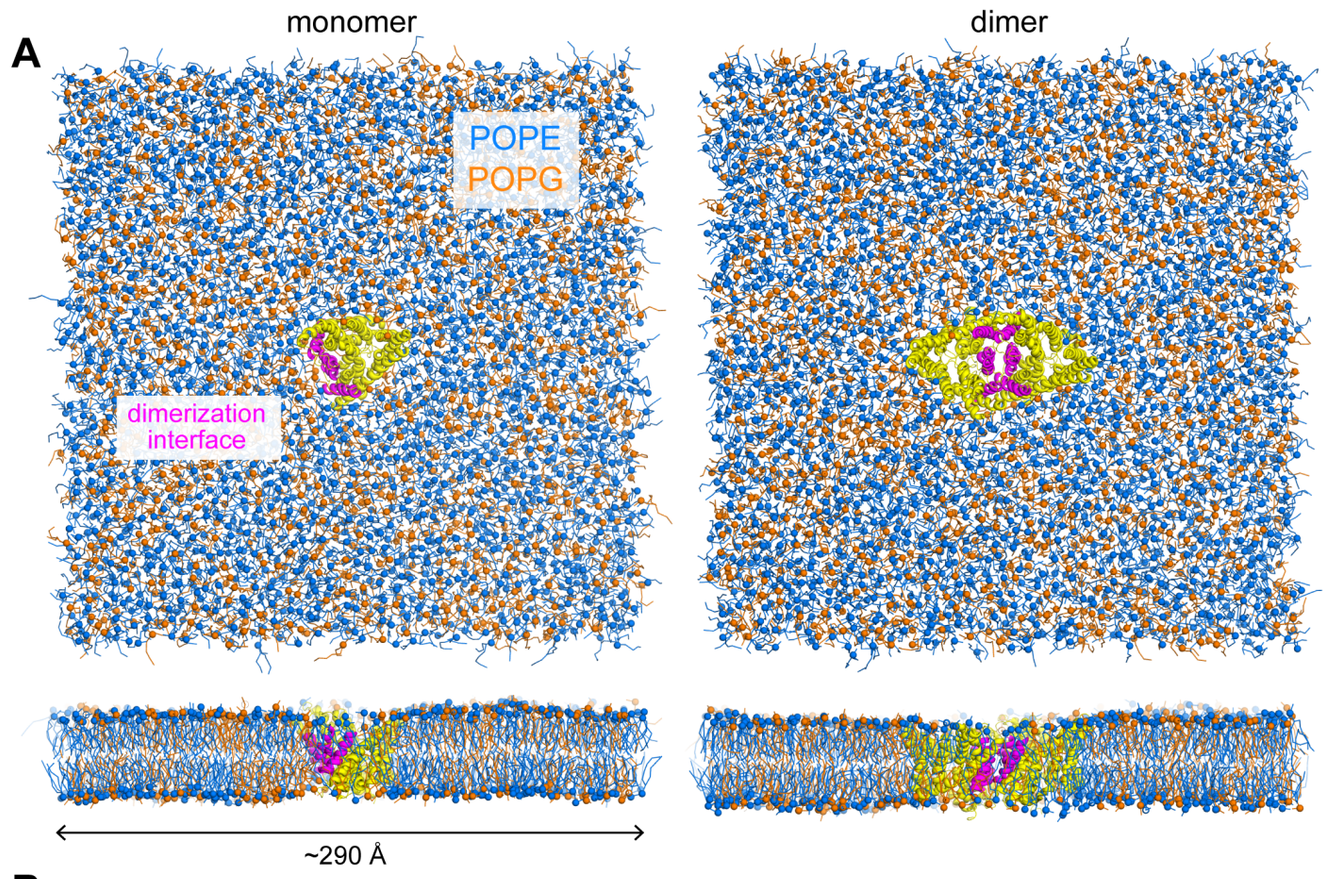

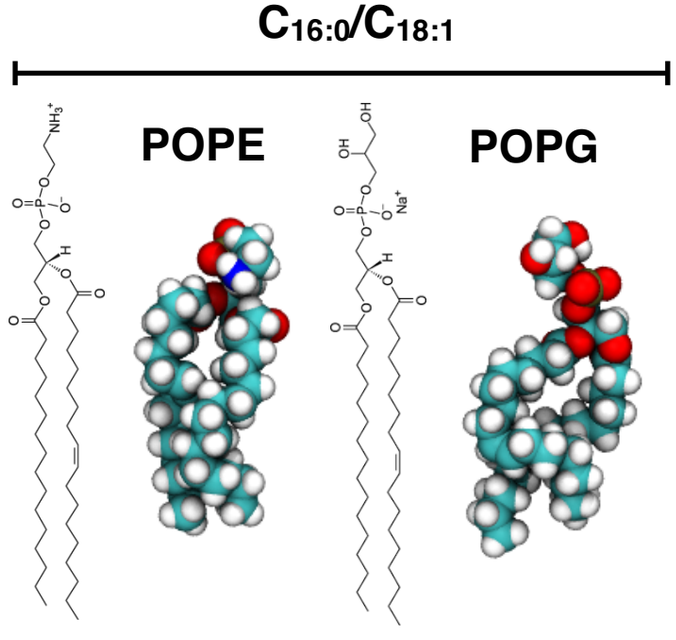

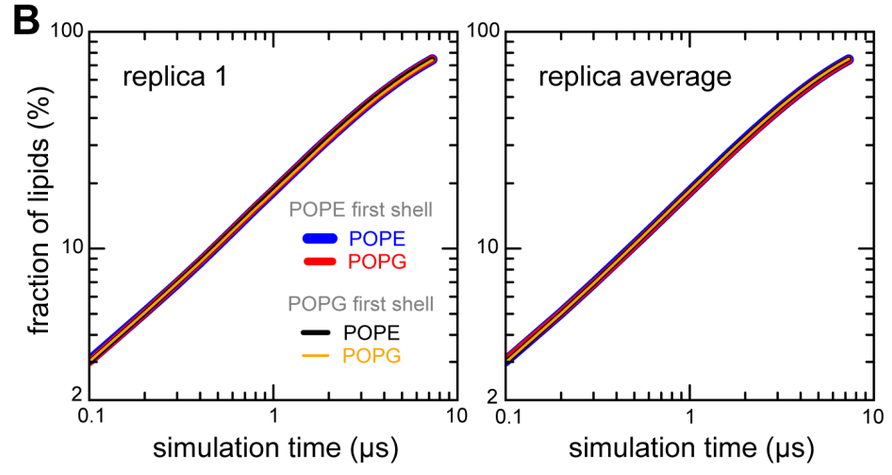

Chadda, Bernhardt, Kelley, Teixeira, Griffith, Gil-Ley, Ozturk, Hughes, Forsythe, Krishnamani, Faraldo-Gómez* & Robertson*, eLife 2021

Molecular dynamics simulations of membranes

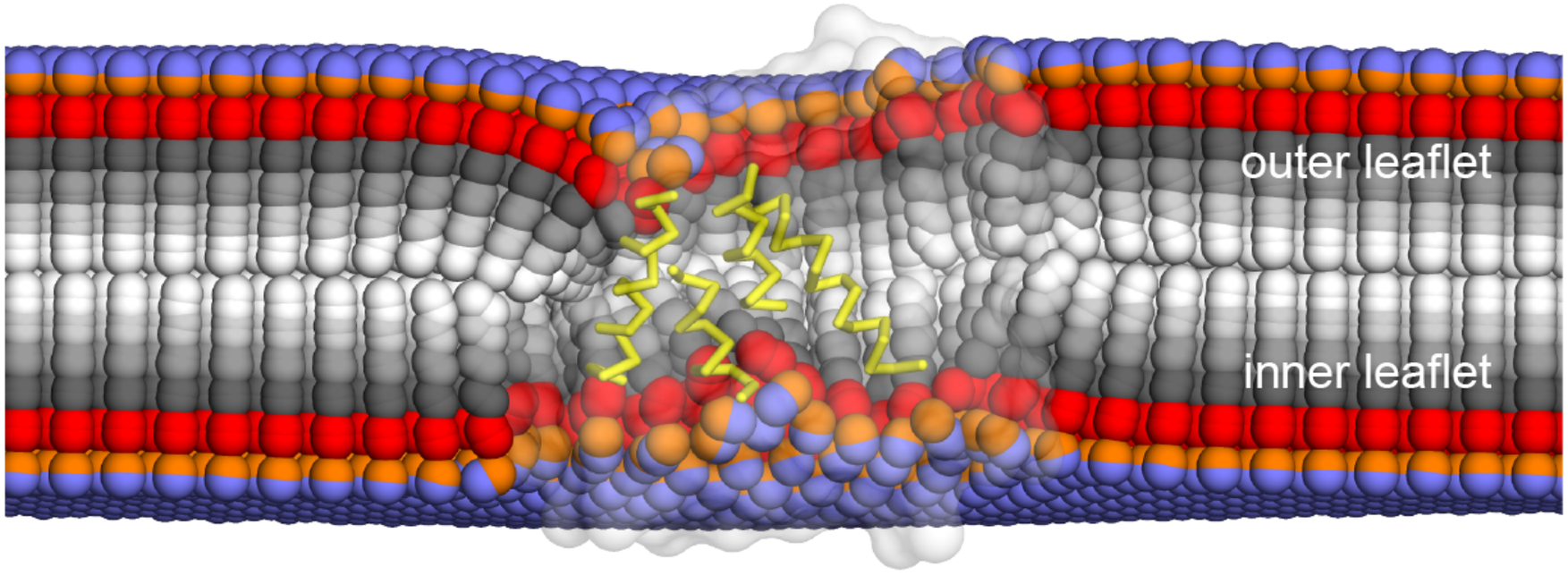

time-averaged lipid structures

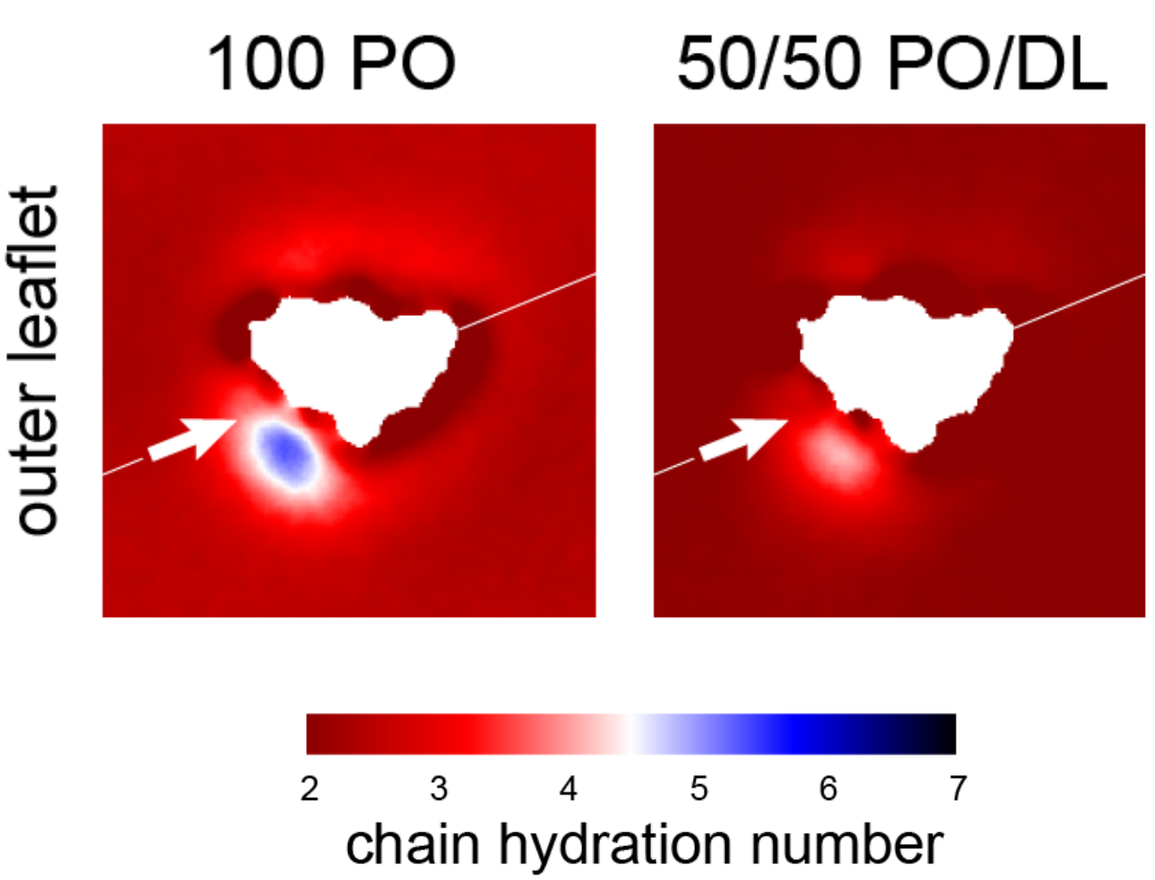

Chadda, Bernhardt, Kelley, Teixeira, Griffith, Gil-Ley, Ozturk, Hughes, Forsythe, Krishnamani, Faraldo-Gómez* & Robertson*, eLife 2021

Lipid configurations can vary in many ways

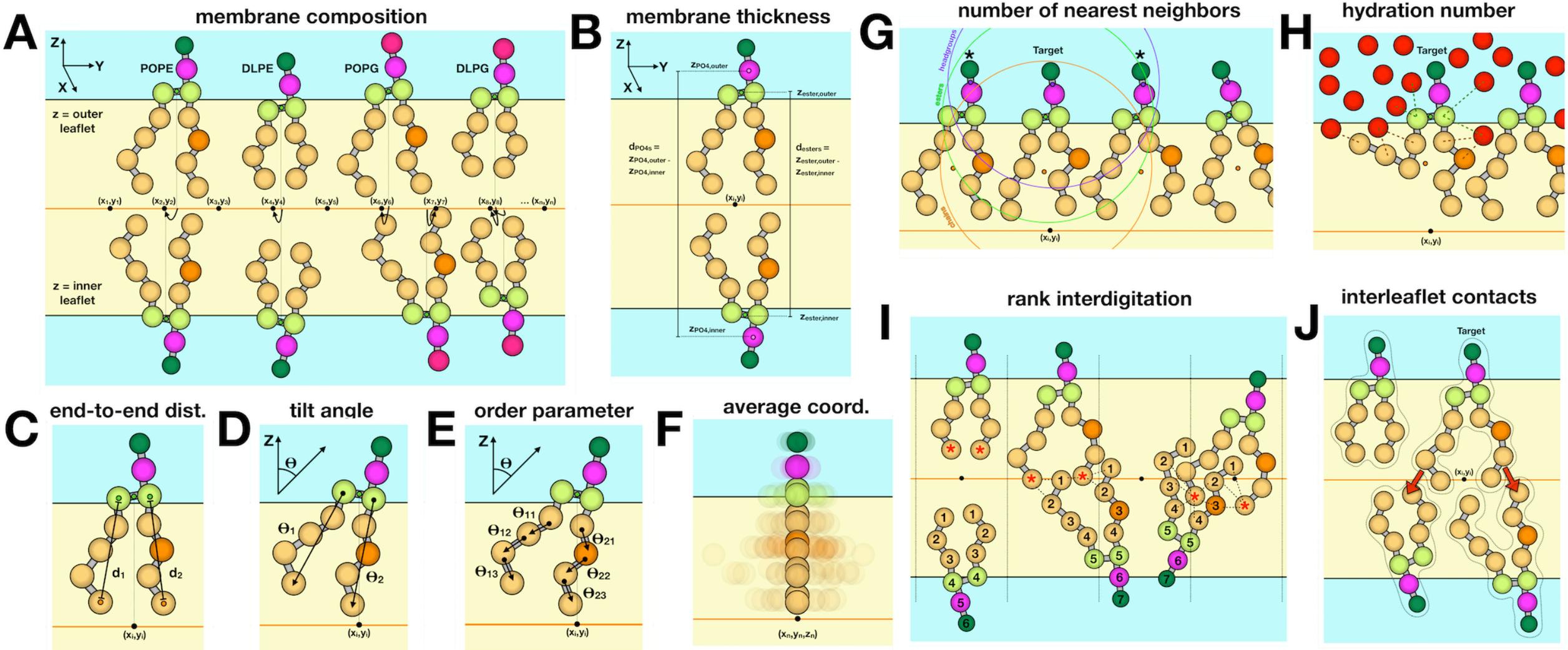

Chadda, Bernhardt, Kelley, Teixeira, Griffith, Gil-Ley, Ozturk, Hughes, Forsythe, Krishnamani, Faraldo-Gómez* & Robertson*, eLife 2021

Methods for analyzing lipid configurations & dynamics

Table 1. Descriptors of membrane structure and dynamics accessible in MOSAICS 1.0 and in other simulation analysis tools[‡]

	MOSAICS	LiPyphilic	LoMePro	APL*Voro	LipidDyn	Grid-MAT	LOOS	Membrainy	MEMB-PLUGIN	MemSurfer
Bilayer shape	Yes	Yes	----	----	----	----	Yes	----	----	Yes
Bilayer thickness	Yes	Yes	Yes	Yes	----	Yes	----	Yes	Yes	Yes
Lipid-chain order parameter*	Yes	Yes	Yes	----	----	----	Yes	----	----	----
Area per lipid*	Yes	Yes	Yes	Yes	----	----	----	----	----	Yes
Multicomponent lipid enrichment*	Yes	----	----	----	Yes	----	----	----	----	----
Lipid density*	Yes	----	----	----	Yes	----	Yes	Yes	Yes	Yes
Mean lipid tilt*,§	Yes	----	----	----	----	----	Yes	----	----	----
Mean instantaneous lipid tilt*,§	Yes	Yes	----	----	----	----	----	----	----	----
Leaflet interdigitation	Yes	----	----	----	----	----	----	----	----	----
Interleaflet contacts*	Yes	----	----	----	----	----	----	----	----	----
Lipid-chain end-to-end length*	Yes	----	----	----	----	----	----	----	----	----
Lipid-chain splay*	Yes	----	----	----	----	----	----	----	----	----
Lipid-solvent contacts*	Yes	----	----	----	----	----	----	----	----	----
Lipid-protein H-bond & salt-bridges	Yes	----	----	----	----	----	----	----	----	----
Average lipid conformation*	Yes	----	----	----	----	----	----	----	----	----
Lipid radius of gyration	Yes	----	----	----	----	----	----	----	----	----
Lipid residence time	Yes	----	----	----	----	----	----	----	----	----
Multicomponent lipid mixing	Yes	----	----	----	----	----	----	Yes	----	----
Lipid self-diffusion coefficients	Yes	Yes	----	----	----	----	----	----	----	----
Lipid solvation-shell on/off rates	Yes	----	----	----	----	----	----	Yes	----	----
Lipid flipping	Yes	Yes	----	----	----	----	----	----	----	----
Membrane protein tilt angle	Yes	----	----	----	----	----	----	----	----	----
Parallelization	MPI	----	----	----	Multi-core	----	Multi-core	Multi-core	----	----
Supported trajectory file format	GROMACS	Multiple	GROMACS	GROMACS	GROMACS	GROMACS	Multiple	GROMACS	Multiple	Multiple
Programming language	C++	Python	C	C++	Python	Perl	C++	Java	TCL	C++/Python

([‡]) In MOSAICS 1.0, most descriptors are provided as 2D spatial distributions across the membrane plane, which can be represented as heat maps filtered by user-defined statistical-significance thresholds; selected observables (*) are also available as 3D distributions. Only self-diffusion coefficients and lipid-mixing are provided as global average properties. Descriptors available in other software tools but not in MOSAICS 1.0 are not included in this table, for conciseness; we refer the reader to the corresponding publications for further details. ([§]) Further details on these alternative definitions are provided below.

Bernhardt N, Faraldo-Gómez JD. MOSAICS: A software suite for analysis of membrane structure and dynamics in simulated trajectories. Biophys J. 2022 Nov 3:S0006-3495(22)00903-1. doi: 10.1016/j.bpj.2022.11.005. Epub ahead of print. PMID: 36333911.

Lipid dynamics are slow

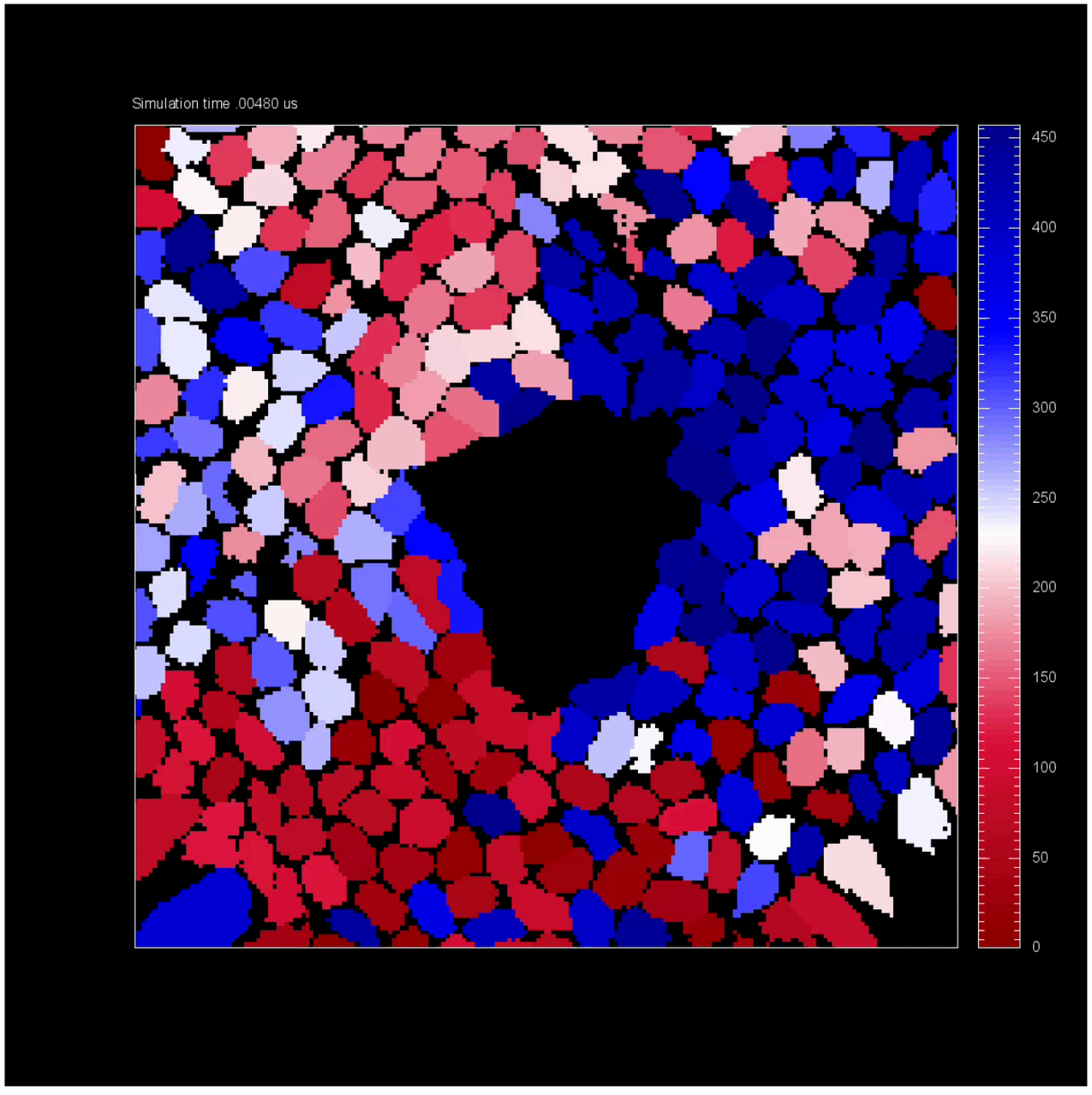

Blue - PO

Red - DL

Molecular dynamics simulations of membranes

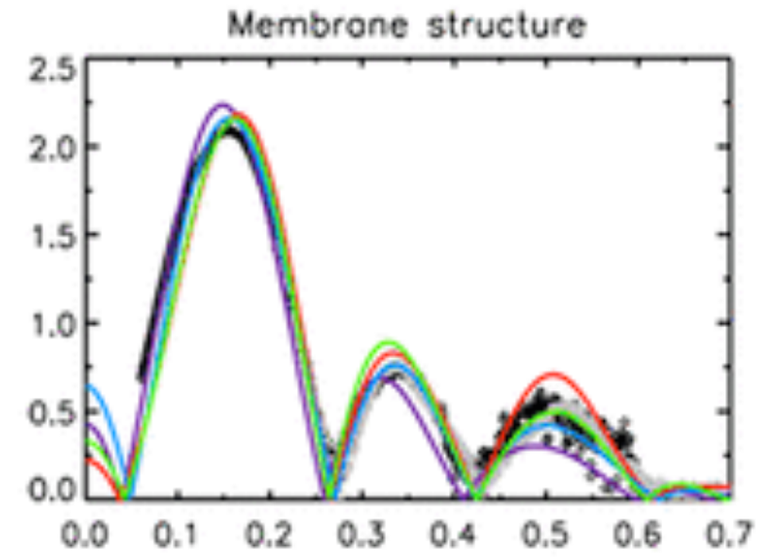

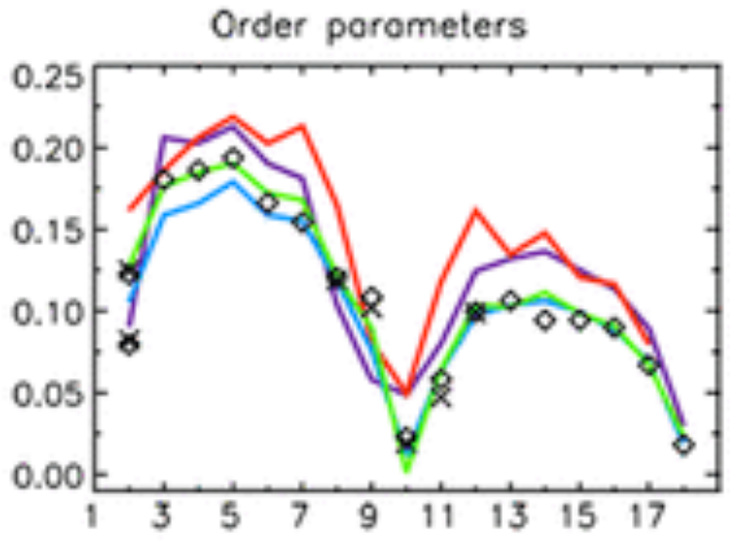

Slipids

Lipid14

?

CHARMM36

GROMOS54a7

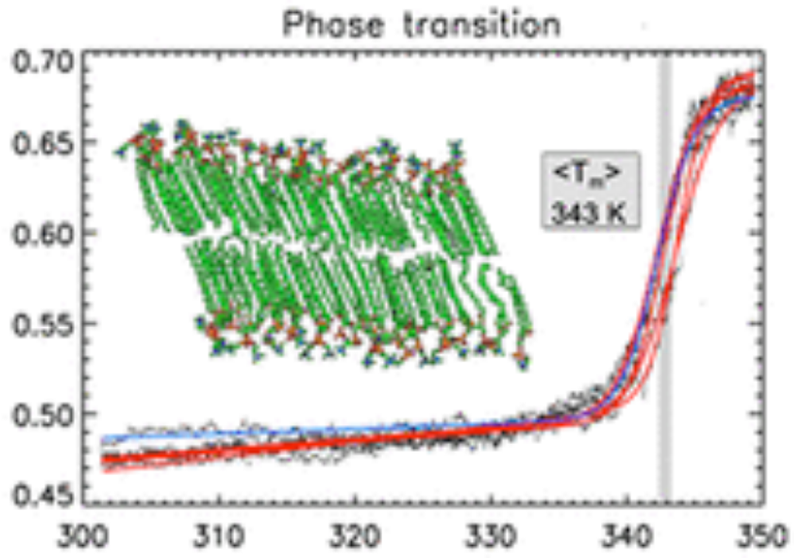

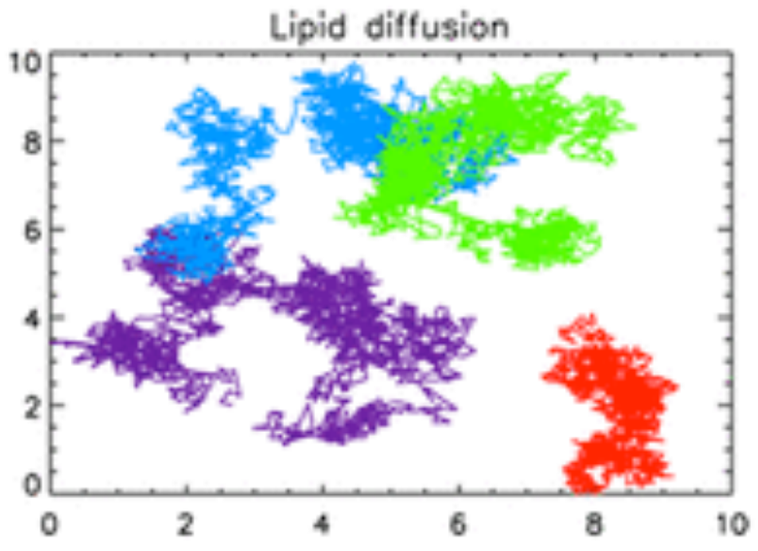

Leonard et al., *Chem. Rev.* 2019, 119, 9, 6227–6269
https://doi.org/10.1021/acs.chemrev.8b00384

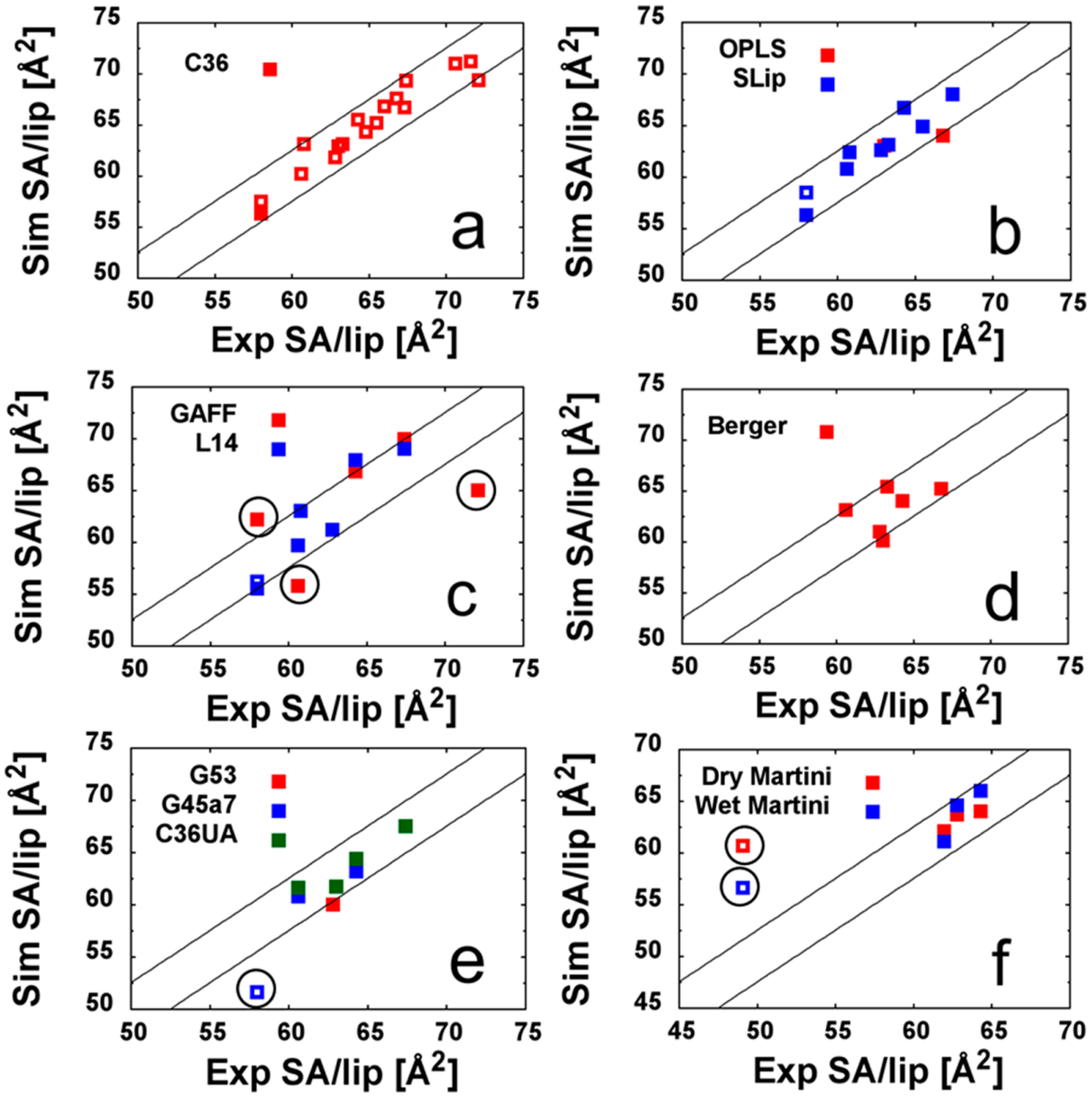

Figure 5. SA/lip obtained from simulation are compared with experiment for various FFs.[42,75,107,109,110,112,113,120,126,181,188,189,191,206,313−318] Solid and empty squares are PC and PE lipids, respectively. Black diagonal lines represent the 95% confidence intervals of the experimental D_{HH}. Outliers are circled for clarity and described in the text. Data from common saturated and monounsaturated lipids are shown.

DOI: 10.1021/acs.chemrev.8b00384
Chem. Rev. 2019, 119, 6227−6269

Biology 5357: Chemistry & Physics of Biomolecules
Fall 2023

Lecture 7:
Membrane proteins: folding and self-assembly

Janice L. Robertson
Dept. of Biochemistry & Molecular Biophysics
McDonnell Sciences Building 223A (Lab 223)
janice.robertson@wustl.edu

Background Reading

Cell Boundaries - How Membranes and Their Proteins Work. Stephen White, Gunnar von Heijne, Donald M. Engelman. CRC Press 2022.

Cell membranes are greasy

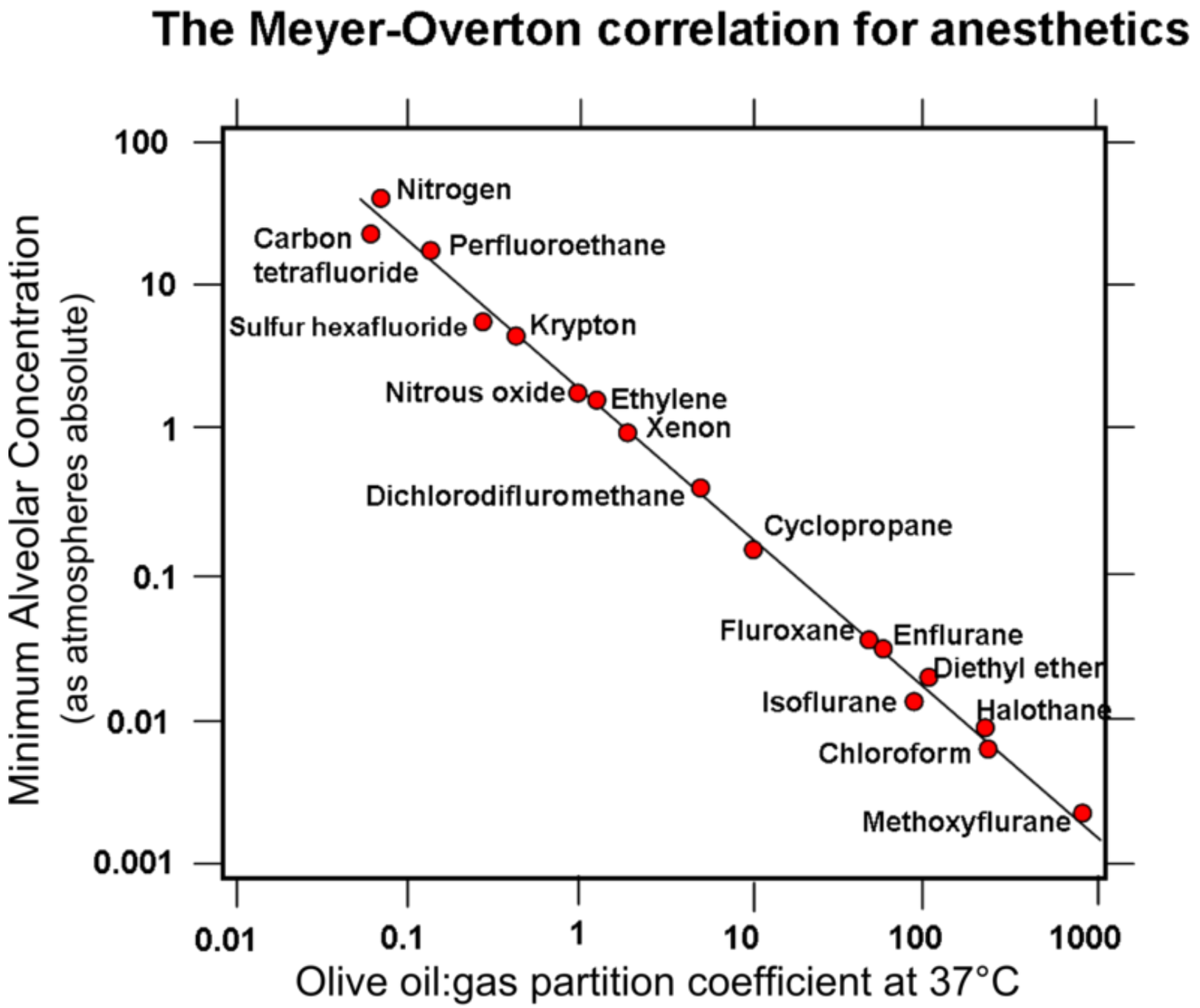

The problem of protein partitioning into membranes

Polypeptides are expected to be unstable in membranes due to unsatisfied charges in the backbone

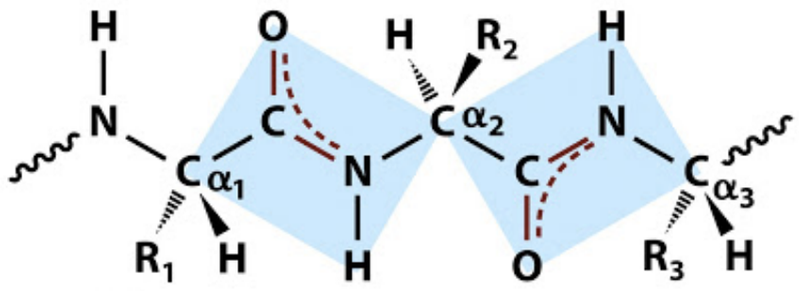

Figure 4-6 Principles of Biochemistry, 4/e
© 2006 Pearson Prentice Hall, Inc.

Davson & Danielli model

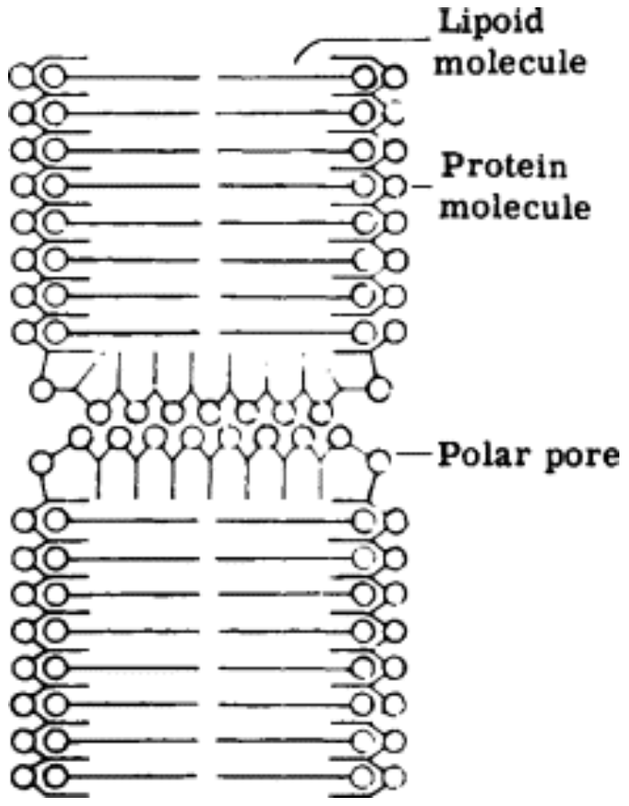

Measurement of free energy of membrane partitioning

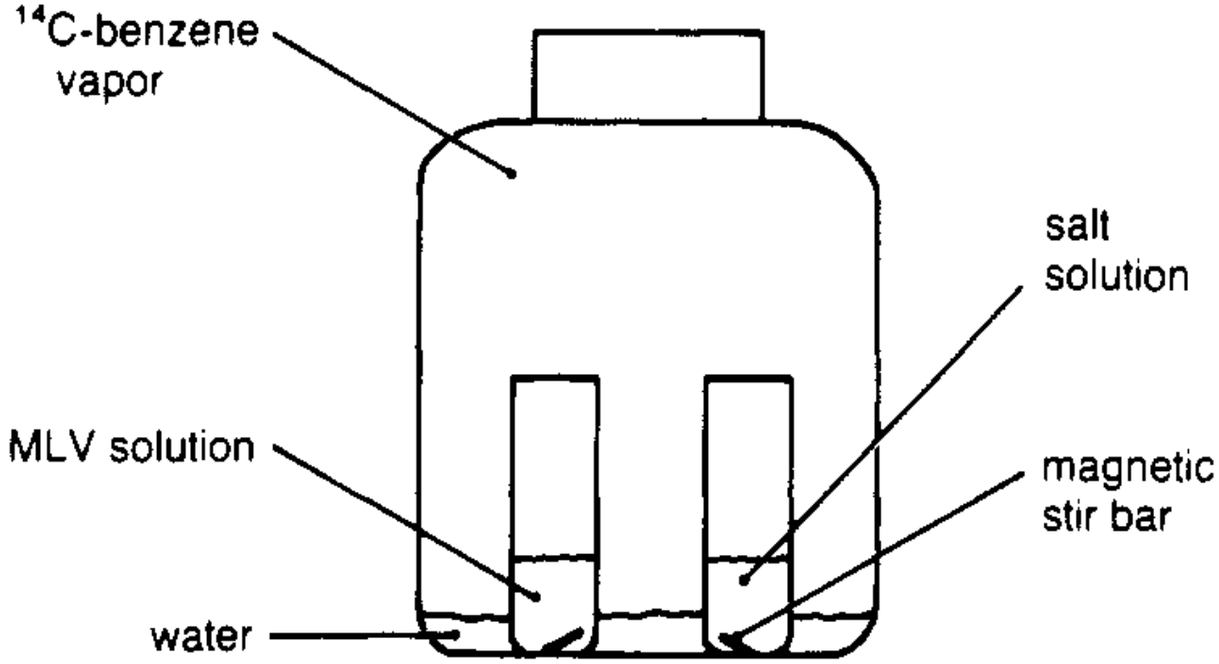

FIGURE 1: Experimental apparatus used to measure partition coefficients. The vesicle solution and corresponding aqueous solution are each placed in a glass vial along with a magnetic stir bar. Water surrounds the vials to facilitate equilibration with the external water bath. Radiolabeled benzene is pipeted into the bottle and equilibrates through the vapor phase. A TFE-lined cap prevents vapor leakage. The bottles are placed on a magnetic stirrer, submerged in a water bath, and incubated at fixed temperature.

$$\Delta G^\circ = \mu_{0,bilayer} - \mu_{0,buffer}$$
$$= -RT \ln K_X$$

$$K_X = X_{bilayer}/X_{buffer}$$
$$= \frac{[P]_{bilayer}/([L]+[P]_{bilayer})}{[P]_{buffer}/([W]+[P]_{buffer})}$$

Partitioning free energies of the peptide backbone

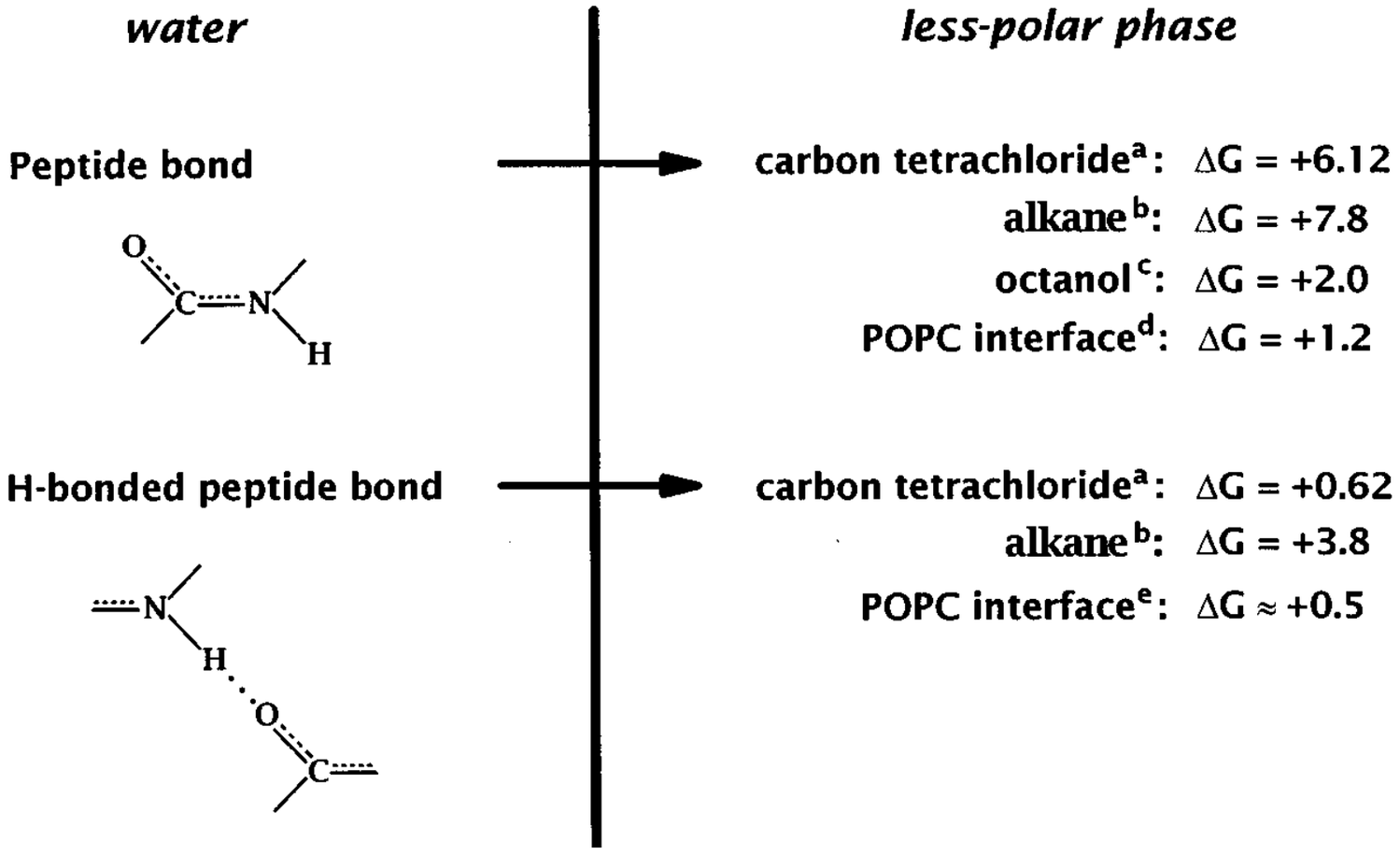

H-bonded secondary structures in membranes

secondary structures

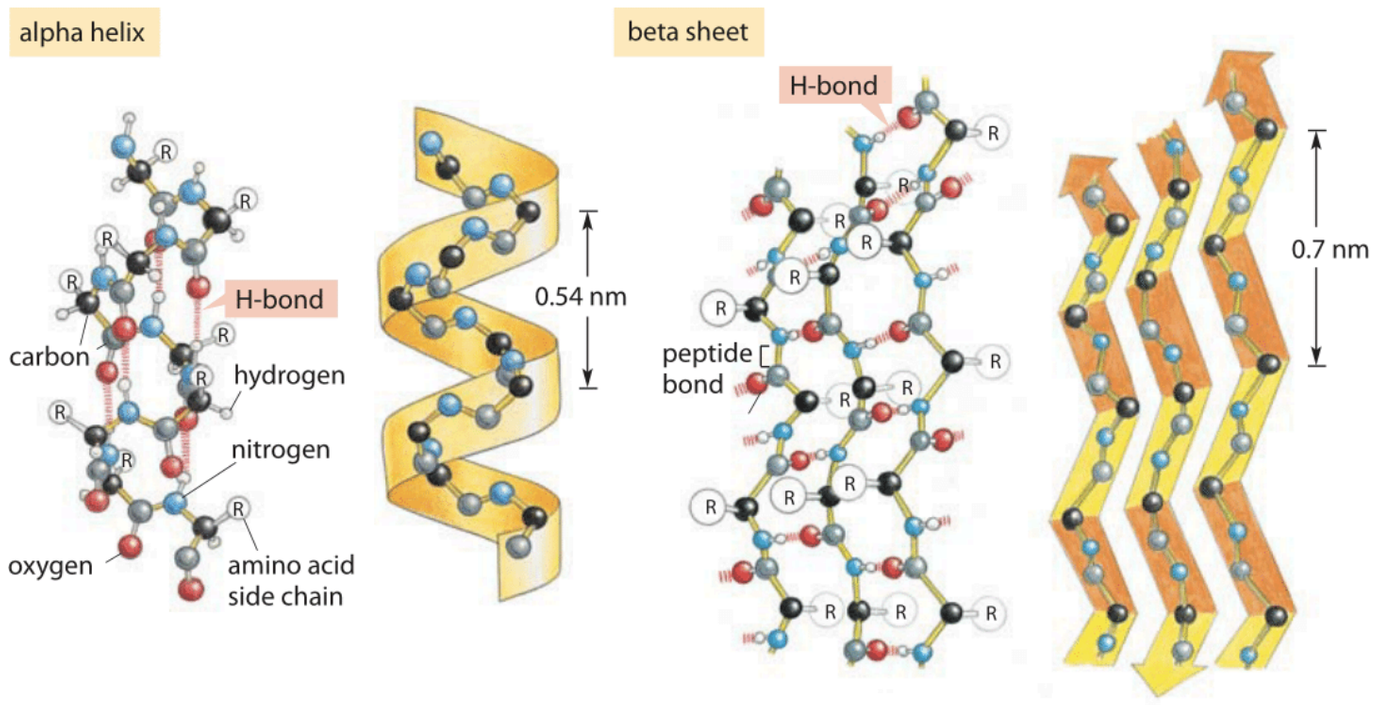

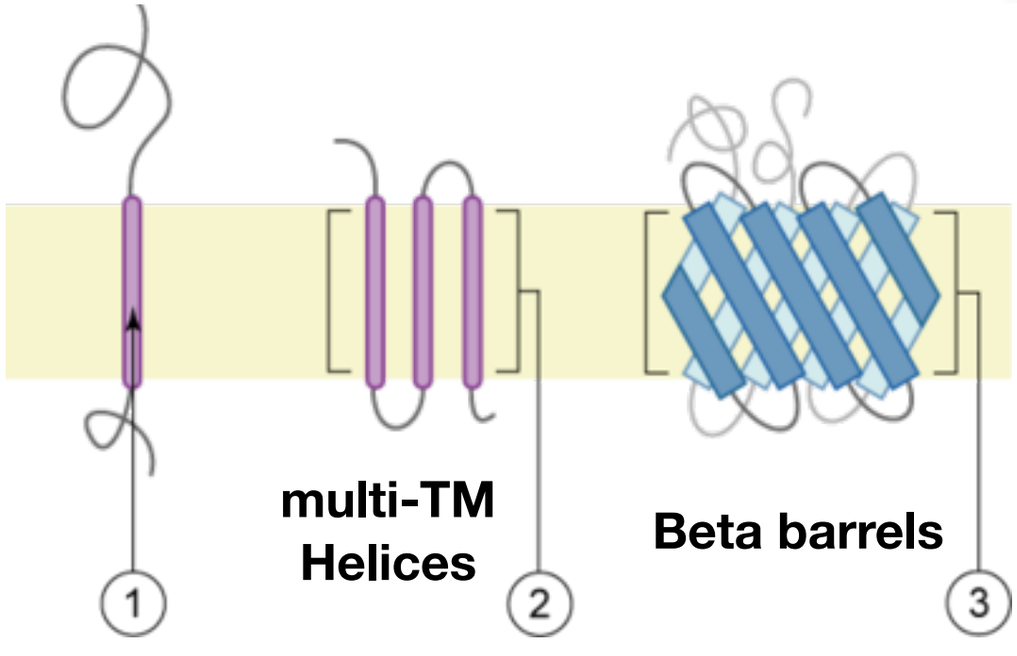

But what about the cost of side-chain partitioning?

SMALL

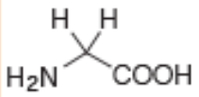

Glycine (Gly, G)
MW: 75.07

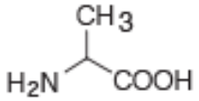

Alanine (Ala, A)
MW: 89.09

NUCLEOPHILIC

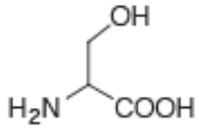

Serine (Ser, S)
MW: 105.09, $pK_a \sim 16$

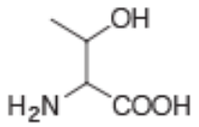

Threonine (Thr, T)
MW: 119.1, $pK_a \sim 16$

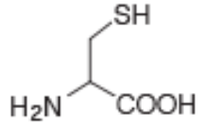

Cysteine (Cys, C)
MW: 121.2, $pK_a = 8.18$

HYDROPHOBIC

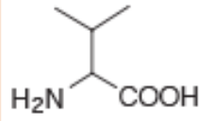

Valine (Val, V)
MW: 117.1

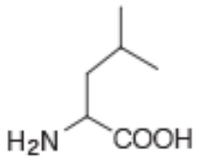

Leucine (Leu, L)
MW: 131.2

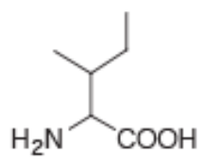

Isoleucine (Ile, I)
MW: 131.2

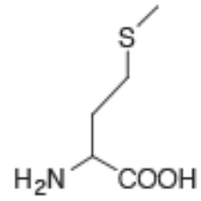

Methionine (Met, M)
MW: 149.2

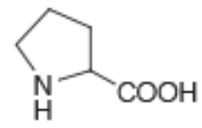

Proline (Pro, P)
MW: 115.1

AROMATIC

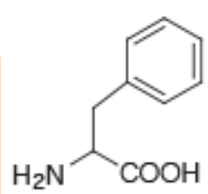

Phenylalanine (Phe, F)
MW: 165.2

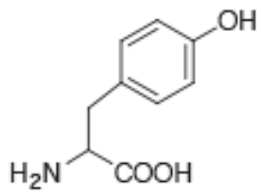

Tyrosine (Tyr, Y)
MW: 181.2, $pK_a = 10.46$

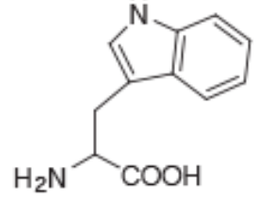

Tryptophan (Trp, W)
MW: 204.2

ACIDIC

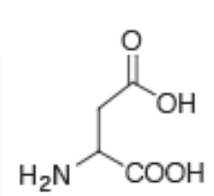

Aspartic Acid (Asp, D)
MW: 133.1, $pK_a = 3.9$

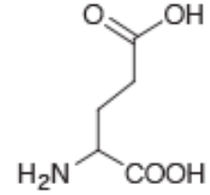

Glutamic Acid (Glu, E)
MW: 147.1, $pK_a = 4.07$

AMIDE

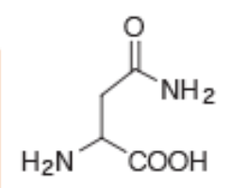

Asparagine (Asn, N)
MW: 132.1

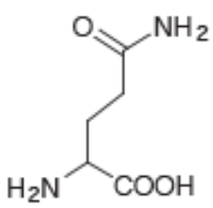

Glutamine (Gln, Q)
MW: 146.1

BASIC

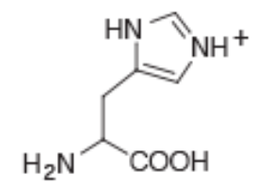

Histidine (His, H)
MW: 155.2, $pK_a = 6.04$

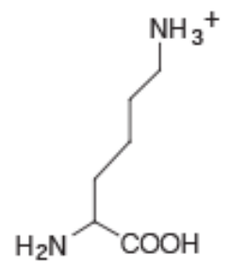

Lysine (Lys, K)
MW: 146.2, $pK_a = 10.79$

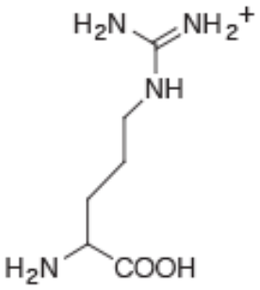

Arginine (Arg, R)
MW: 174.2, $pK_a = 12.48$

Amino Acid side-chain transfer free energies

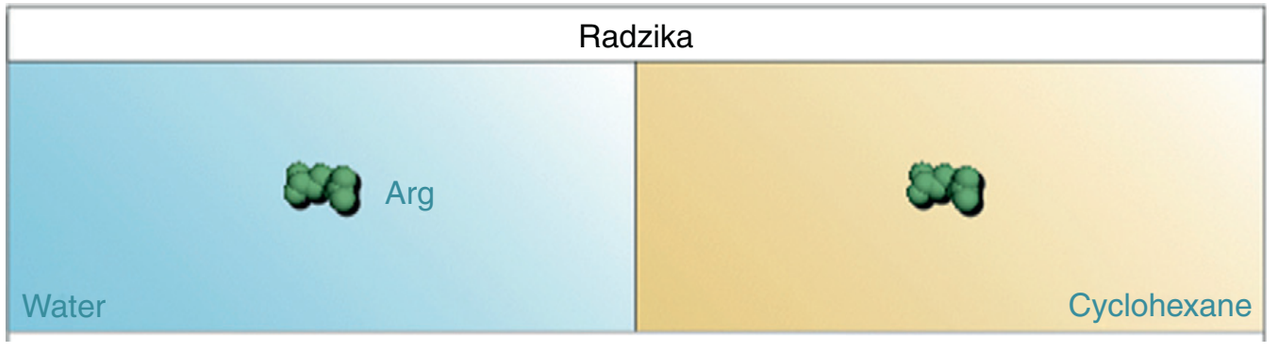

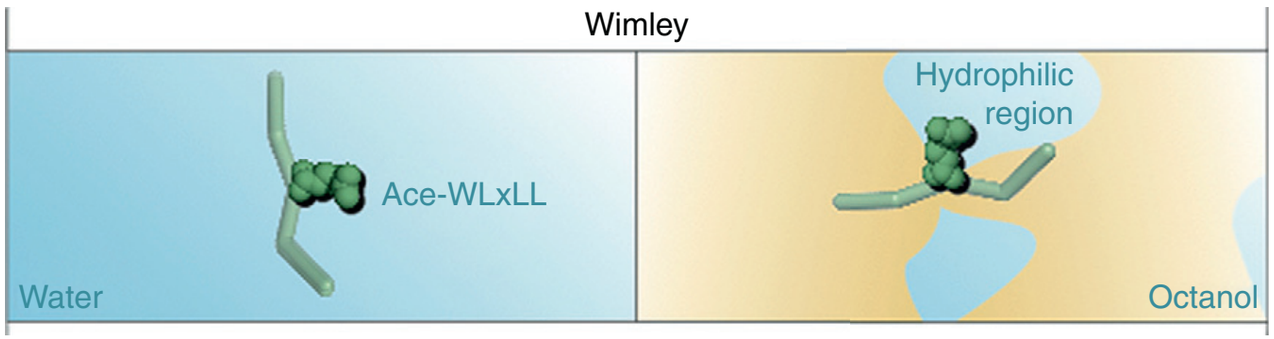

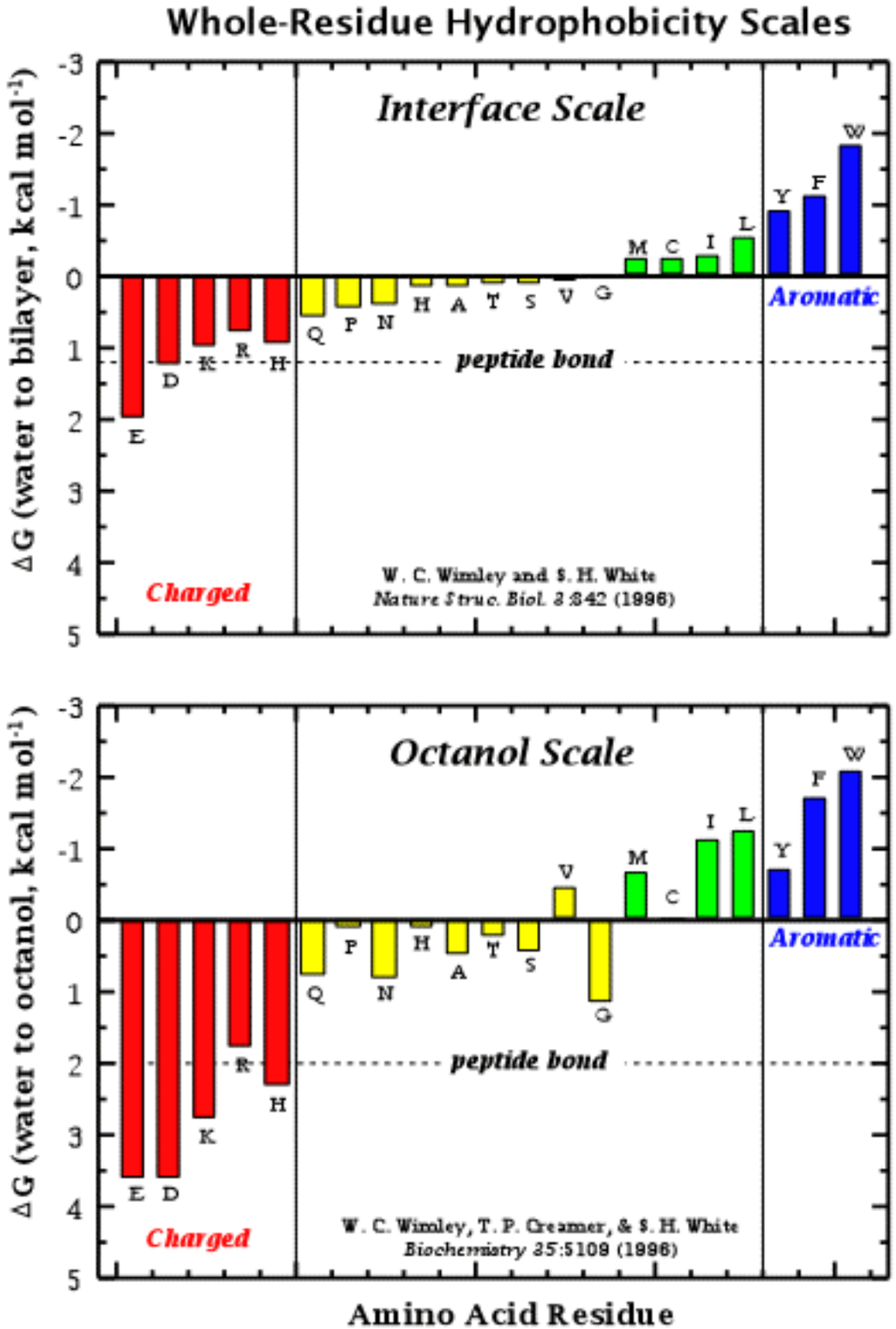

The lipid bilayer is not an isotropic solvent

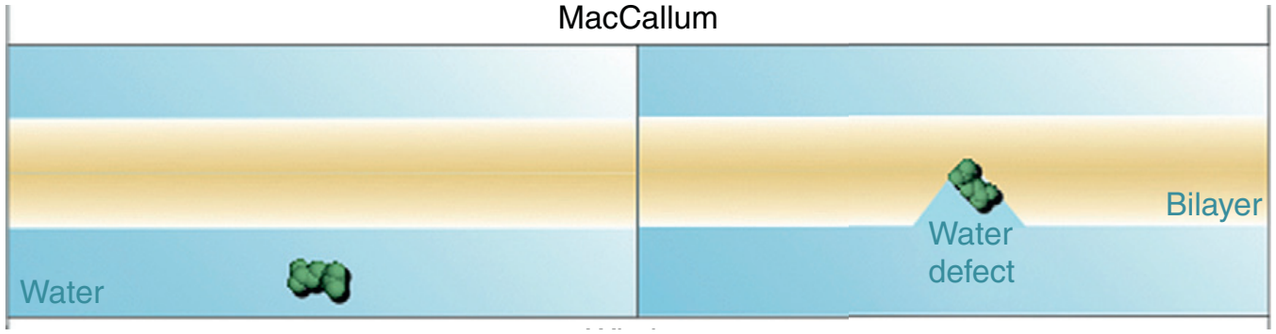

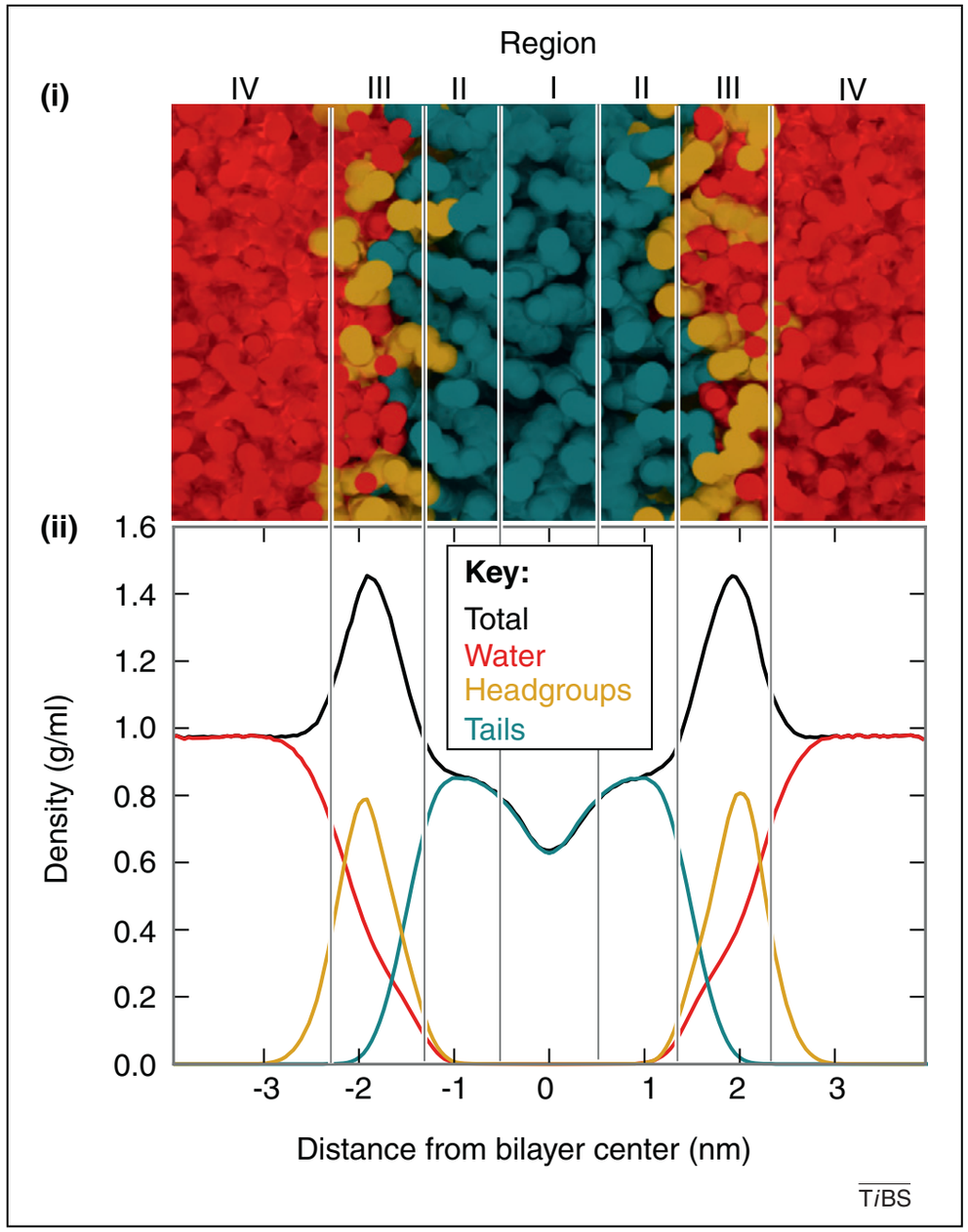

Figure 1. Lipid bilayers contain large variations in density and polarity on a nanometer scale. **(i)** Snapshot of a DOPC bilayer. **(ii)** Partial density profile of a pure DOPC bilayer. The system is divided into four regions with different physicochemical properties [7]. Region I, the center of the bilayer, is hydrophobic and significantly disordered with properties similar to decane. In Region II, the lipid tails are more ordered and have a higher density, similar to a soft polymer. Region III contains a diverse mixture of functional groups including the carbonyl and glycerol groups of the lipid tails, most of the head group density and water. Region IV is defined by water that is perturbed by the lipid bilayer and can be quite deep.

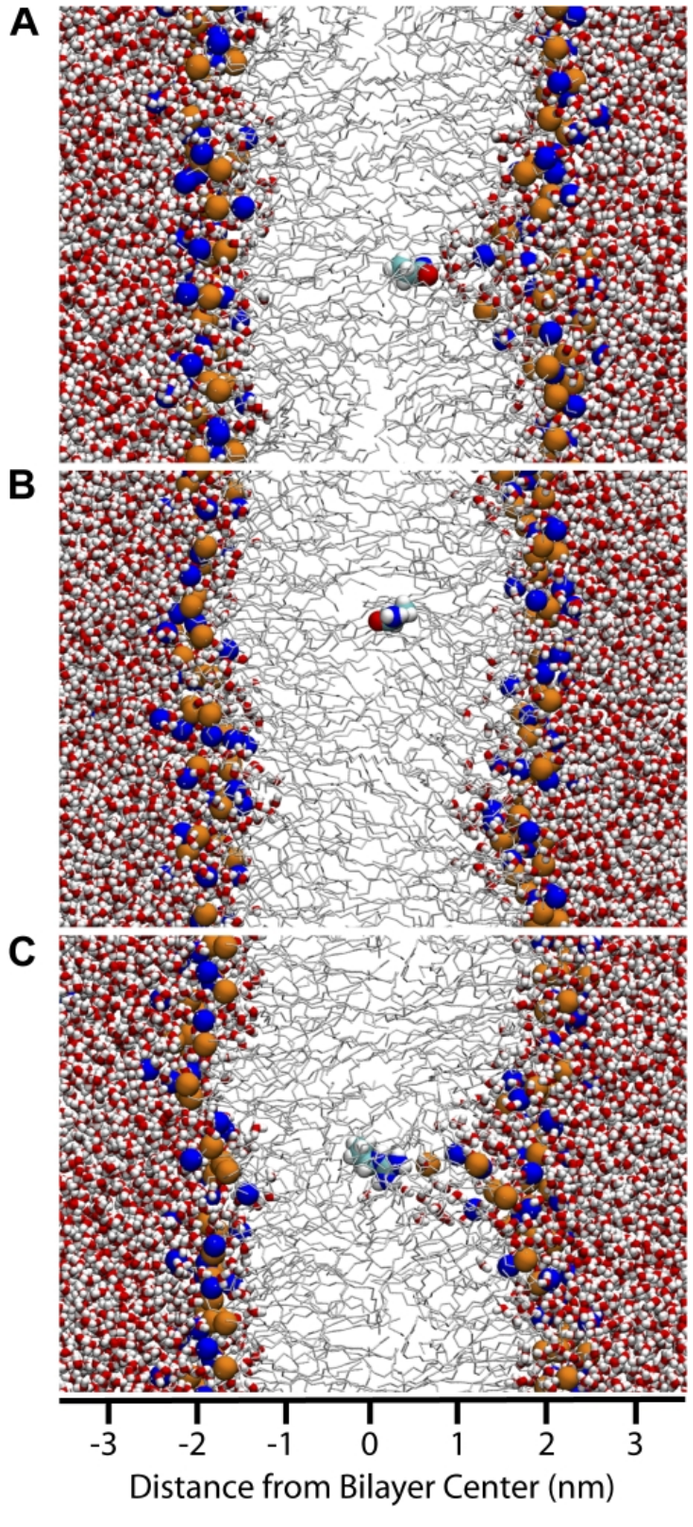
A
B
C
-3
-2
-1
0
1
2
3
Distance from Bilayer Center (nm)

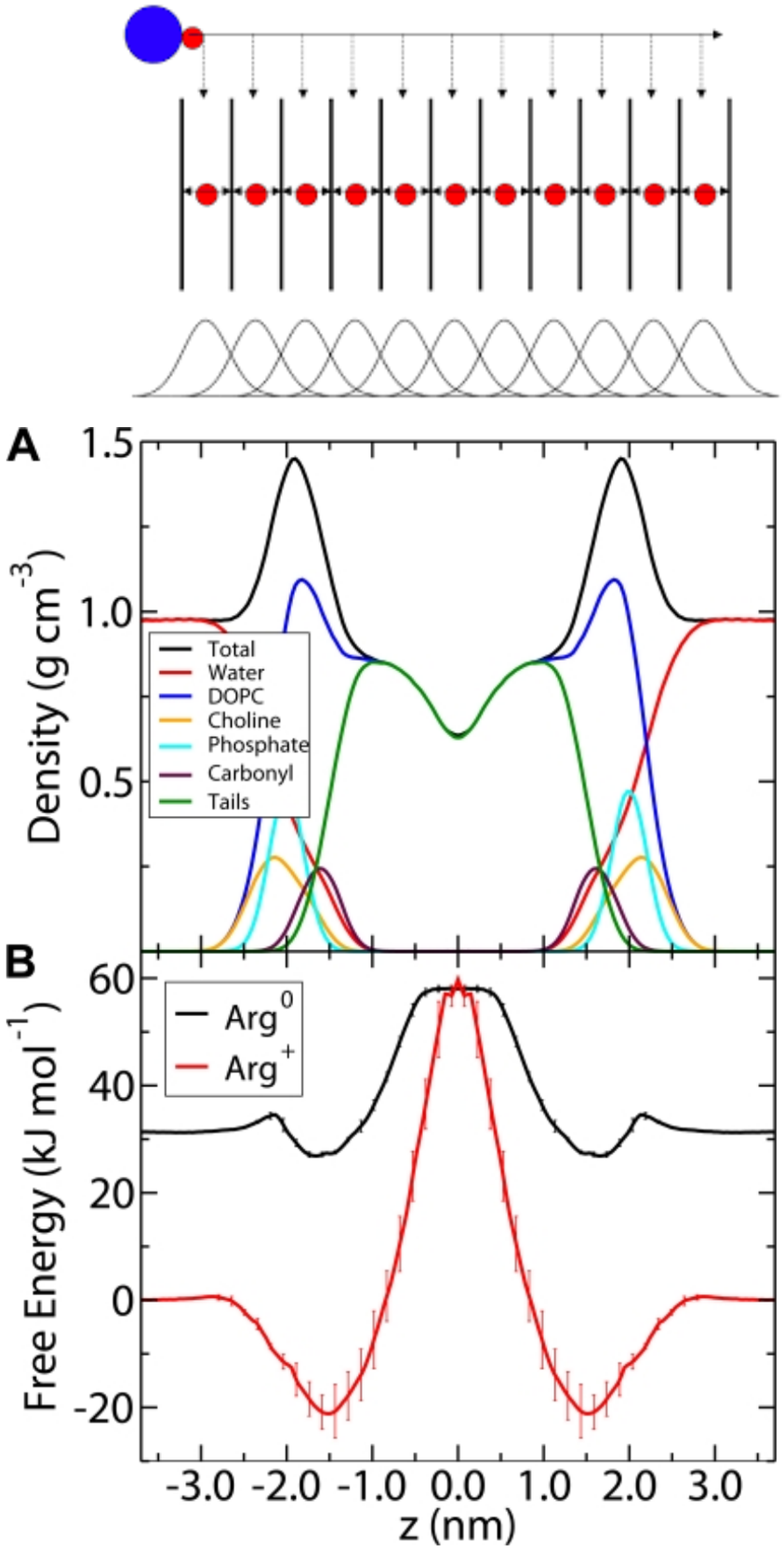
A
1.5
1.0
0.5
Density (g cm-3)
Total
Water
DOPC
Choline
Phosphate
Carbonyl
Tails
B
60
40
20
0
-20
Free Energy (kJ mol-1)
Arg0
Arg+
-3.0 -2.0 -1.0 0.0 1.0 2.0 3.0
z (nm)

The biological translocon scale

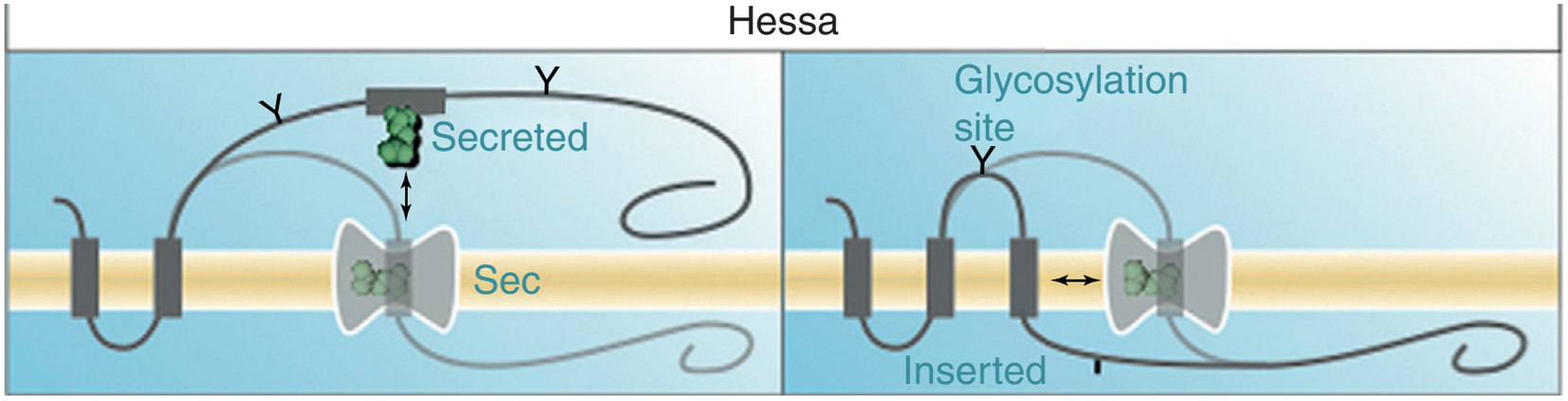

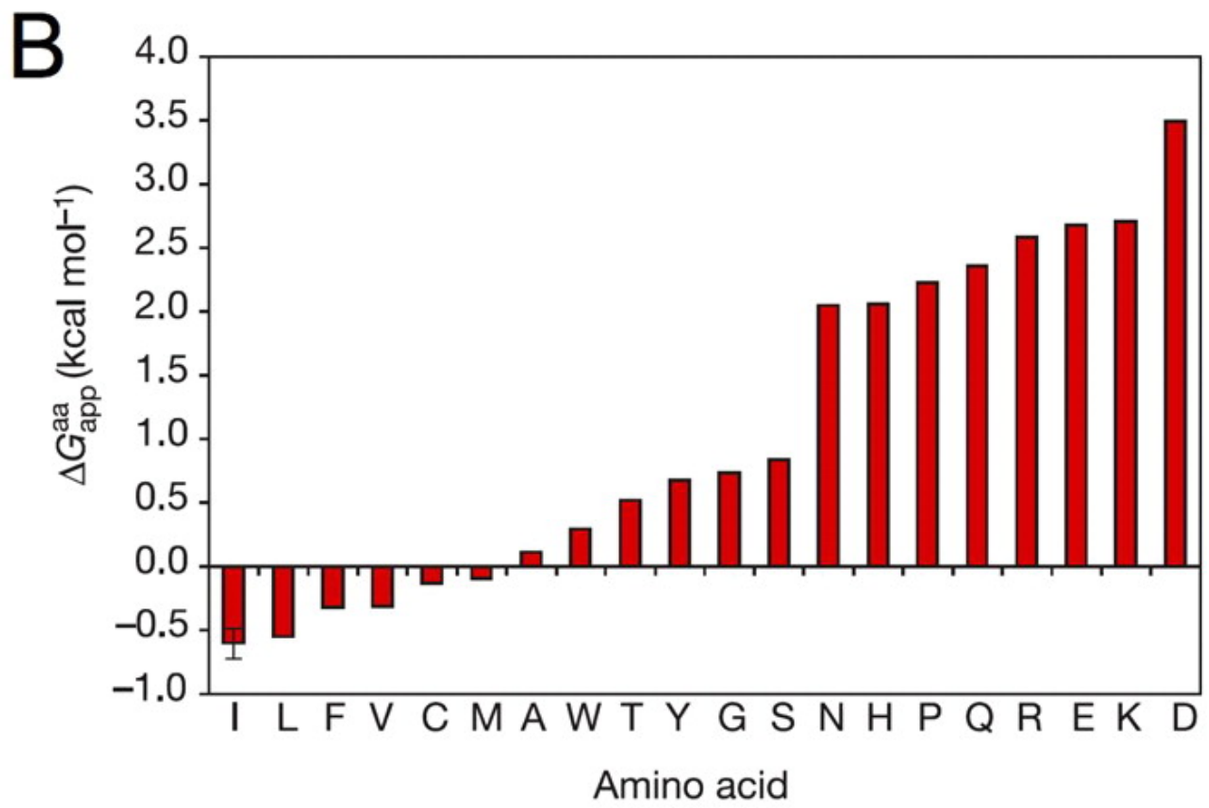

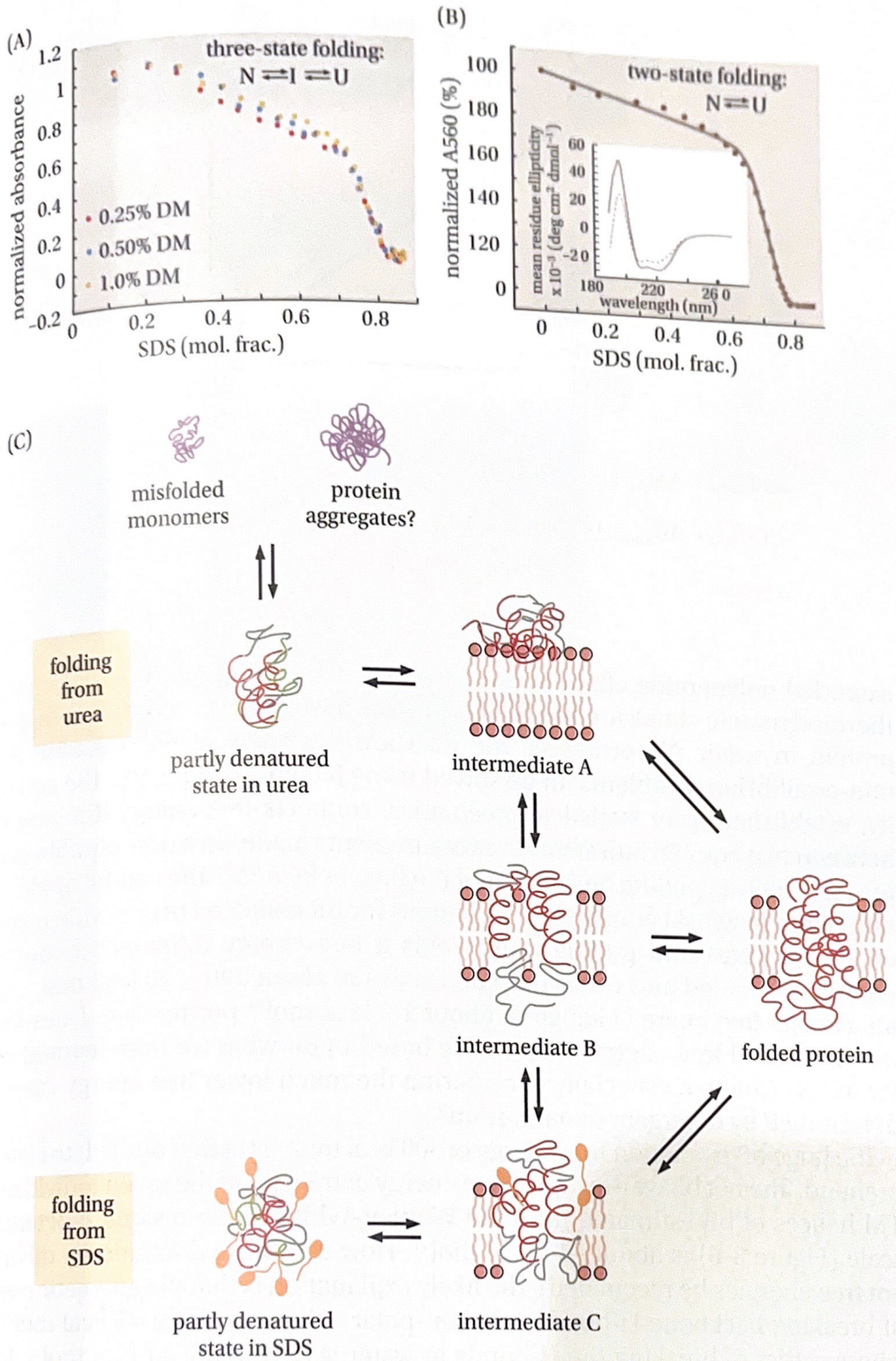

Figure 4.9 Using detergents to unfold membrane proteins. (A) Denaturation curves for diacylglycerol kinase, which has three detectable states. In this case, the refolding is in the presence of the non-denaturing detergent decyl β-D-maltoside (DM). (B) Denaturation of bacteriorhodopsin, which has two states. CD spectra of the two states (inset) show that the denatured state retains most of the helical structure of the native state. (C) A suggested general scheme for folding α-helical membrane proteins out of detergents and urea. (A, From Lau FW, Bowie JU [1997] *Biochemistry* 36: 5884–5892. With permission from the American Chemical Society. B, From Curnow P, Booth PJ [2007] *PNAS* 104: 18970–18975. With permission from PJ Booth. C, From Booth PJ, Curnow P [2006] *Curr Opin Struct Biol* 16: 480–488. With permission from Elsevier.)

Water to lipid bilayer thermodynamics protein folding scale

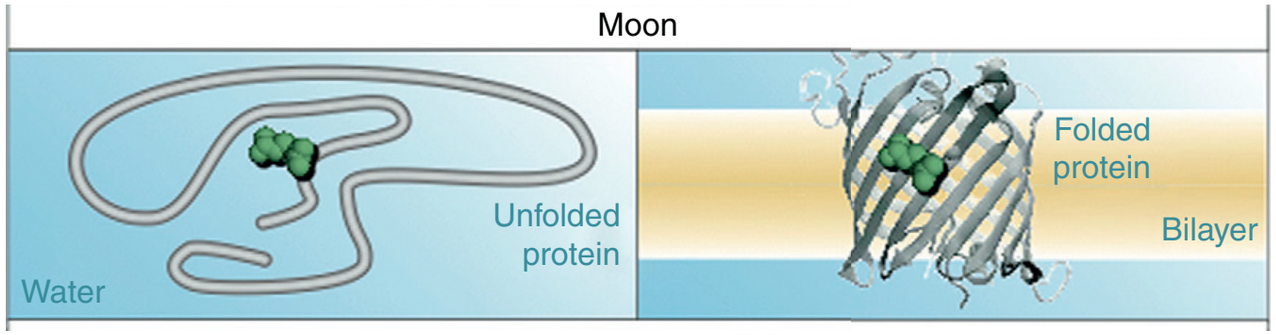

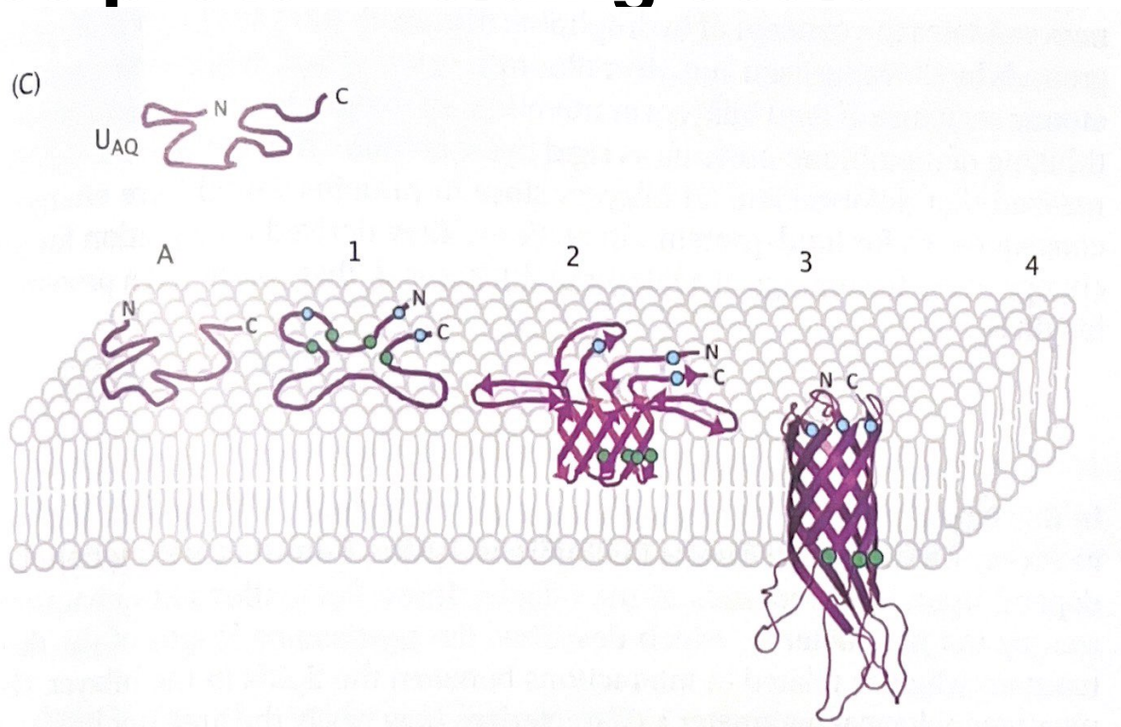

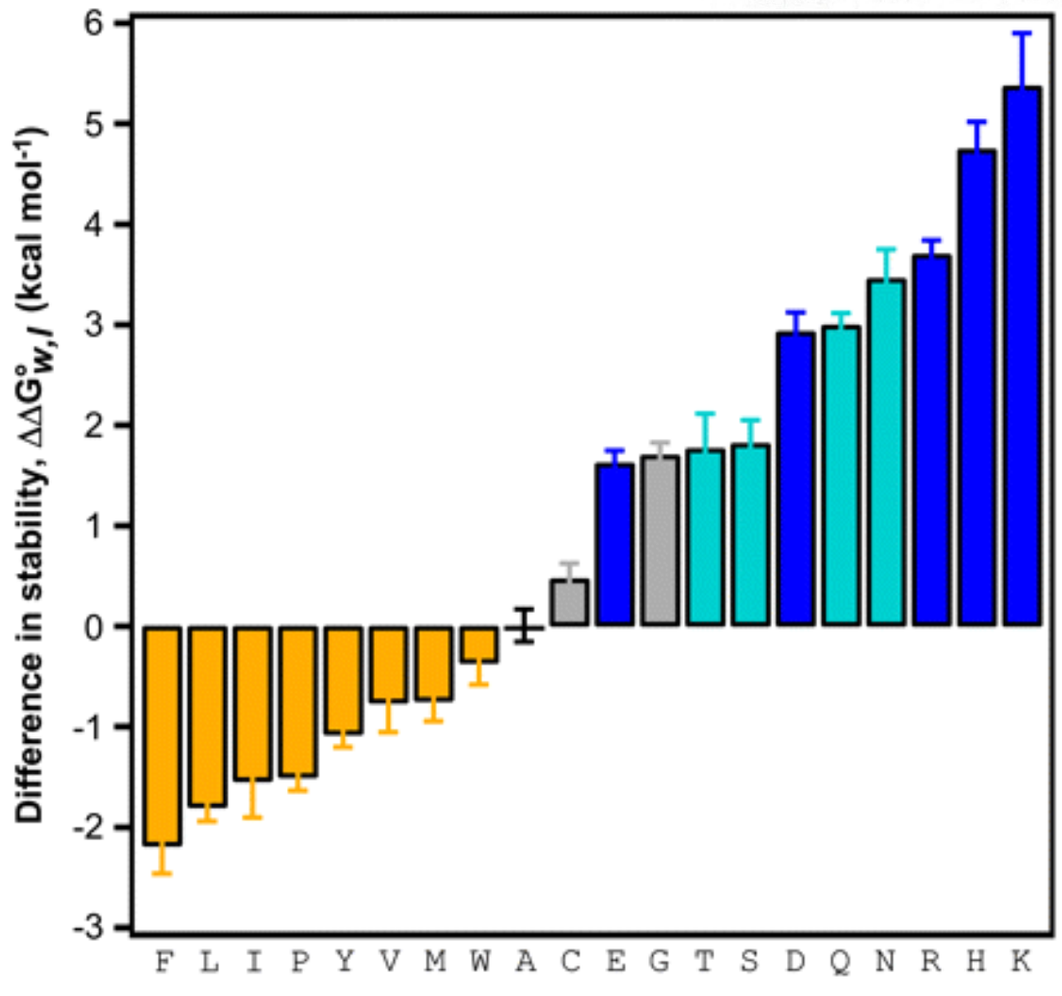

Moon & Fleming, 2010

Depth dependency & cooperatively

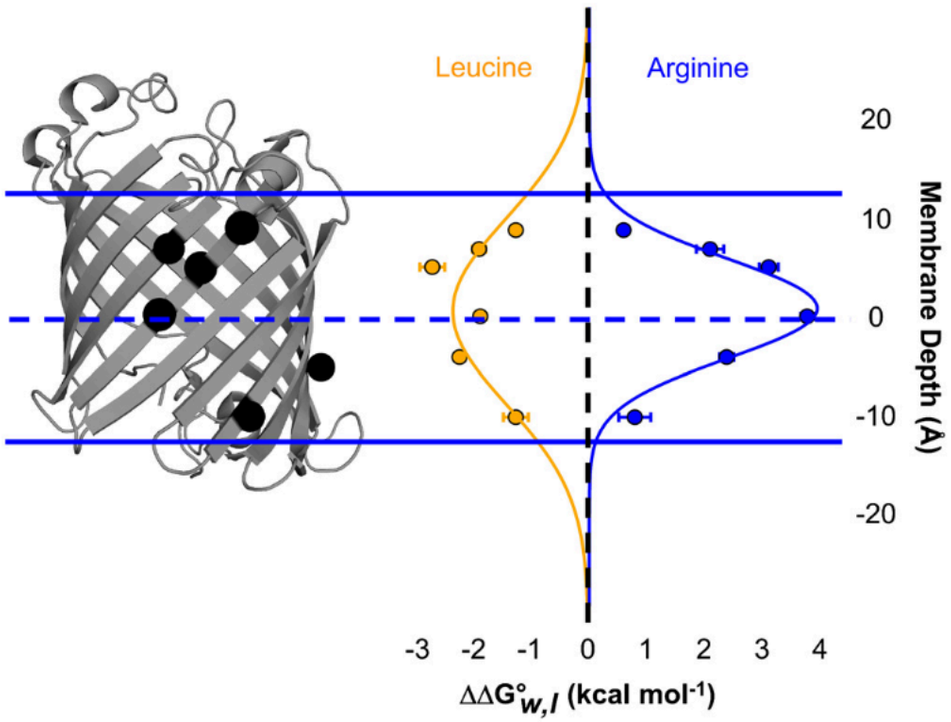

Fig. 3. Energetics of side-chain partitioning varies by depth in the membrane. The OmpLA host-guest system is shown similarly as in Fig. 1 with the α-carbons of sequence positions 120, 164, 210, 212, 214, and 223 shown as black spheres. The membrane depth of those five α-carbons versus the $\Delta\Delta G^{\circ}_{w,l}$ of leucine and arginine variants (compared to alanine variants) is shown aligned with the OmpLA image. Normal distributions fit to the leucine and arginine data are also shown. Error bars represent standard errors of the mean from individual titration experiments.

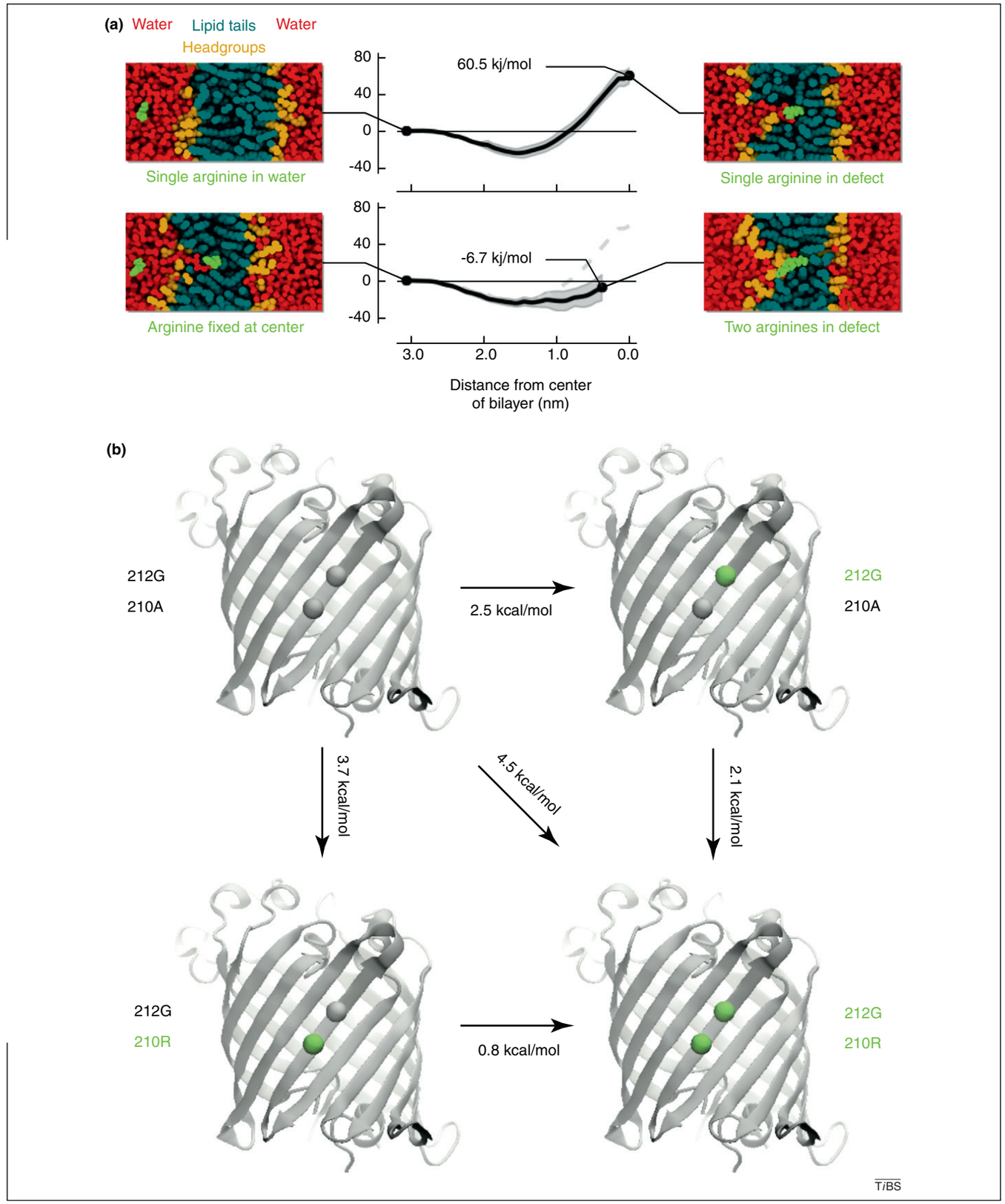

Figure 3. Arginine partitioning into lipid bilayers is non-additive. **(a)** Calculations show that arginine causes a water defect in the membrane. Adding a second arginine to an existing defect causes almost no increase in free energy. Adapted with permission from [47]. **(b)** Experimental observation of non-additivity of arginine partitioning. This panel summarizes five different experimental observations. Adapted with permission from [35].

Amino Acid side-chain transfer free energies

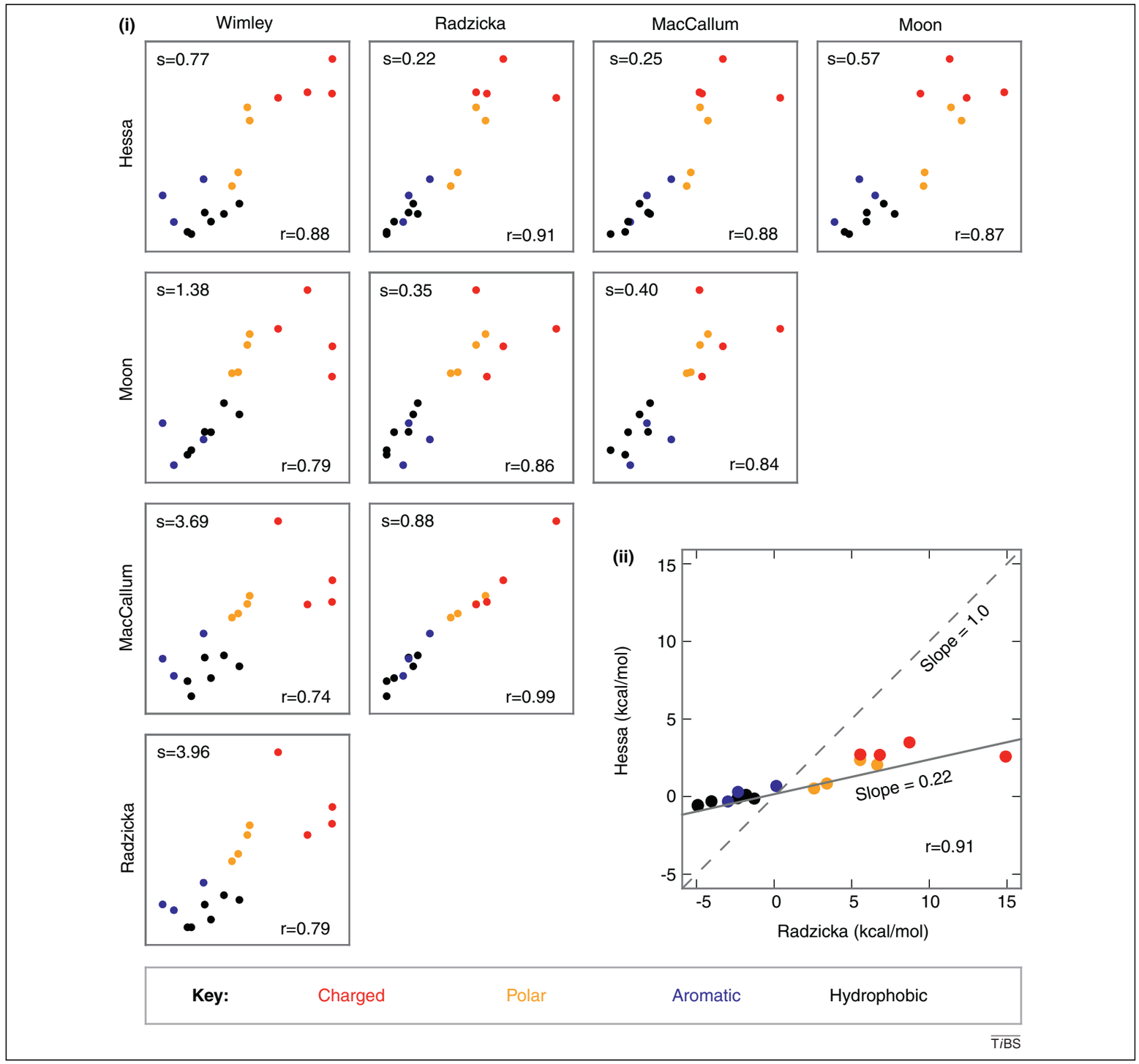

Figure 4. The hydrophobicity scales are correlated but differ in overall magnitude. **(i)** Correlation between the normalized scales. in order to emphasize the correlation (*r*) among the scales; all scales are normalized so that the values range from –1.0 to 1.0. The scales differ in overall magnitude, as indicated by the slope (*s*). **(ii)** Hessa and Radzicka scales are correlated, but differ in overall magnitude scale factor. This panel plots the energies on an absolute scale to emphasize the difference in overall magnitude. Residues are colored by type. His, Pro, Gly were not present in all scales and are not shown. The values for Glu and Asp in Moon might represent a partially neutral state as the experiments were done at pH 3.8.

Hydropathy analysis

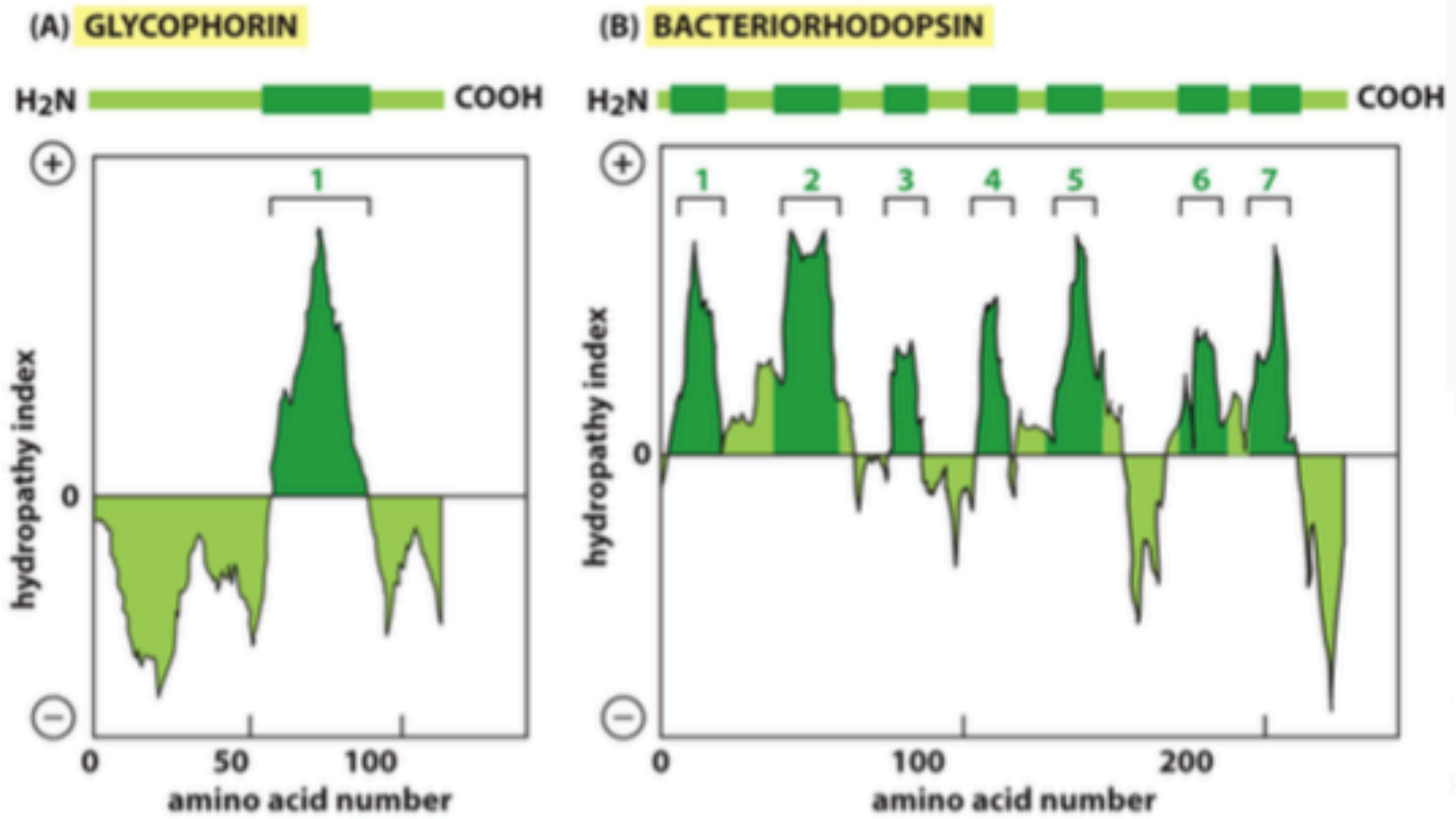

Figure 10-20 Molecular Biology of the Cell 6e (© Garland Science 2015)

Empirical hydrophobicity scales

Figure 3.2 An early hydrophobicity scale for soluble proteins based upon the fraction of each type of amino acid buried in the protein interior or accessible from the aqueous environment. (From Janin J [1979] *Nature* 277: 491–492. With permission from Springer Nature.)

residue	amino acid composition of the inside and surface: molar fraction		free energy (kcal mol^{-1})	
	buried	accessible	f	ΔG_t
Leu	11.7	4.8	2.4	0.5
Val	12.9	4.5	2.9	0.6
Ile	8.6	2.8	3.1	0.7
Phe	5.1	2.4	2.2	0.5
Cys	4.1	0.9	4.6	0.9
Met	1.9	1.0	1.9	0.4
Ala	11.2	6.6	1.7	0.3
Gly	11.8	6.7	1.8	0.3
Trp	2.2	1.4	1.6	0.3
Ser	8.0	9.4	0.8	-0.1
Thr	4.9	7.0	0.7	-0.2
His	2.0	2.5	0.8	-0.1
Tyr	2.6	5.1	0.5	-0.4
Pro	2.7	4.8	0.6	-0.3
Asn	2.9	6.7	0.4	-0.5
Asp	2.9	7.7	0.4	-0.6
Gln	1.6	5.2	0.3	-0.7
Glu	1.8	5.7	0.3	-0.7
Arg	0.5	4.5	0.1	-1.4
Lys	0.5	10.3	0.05	-1.8

The two-stage membrane protein folding model

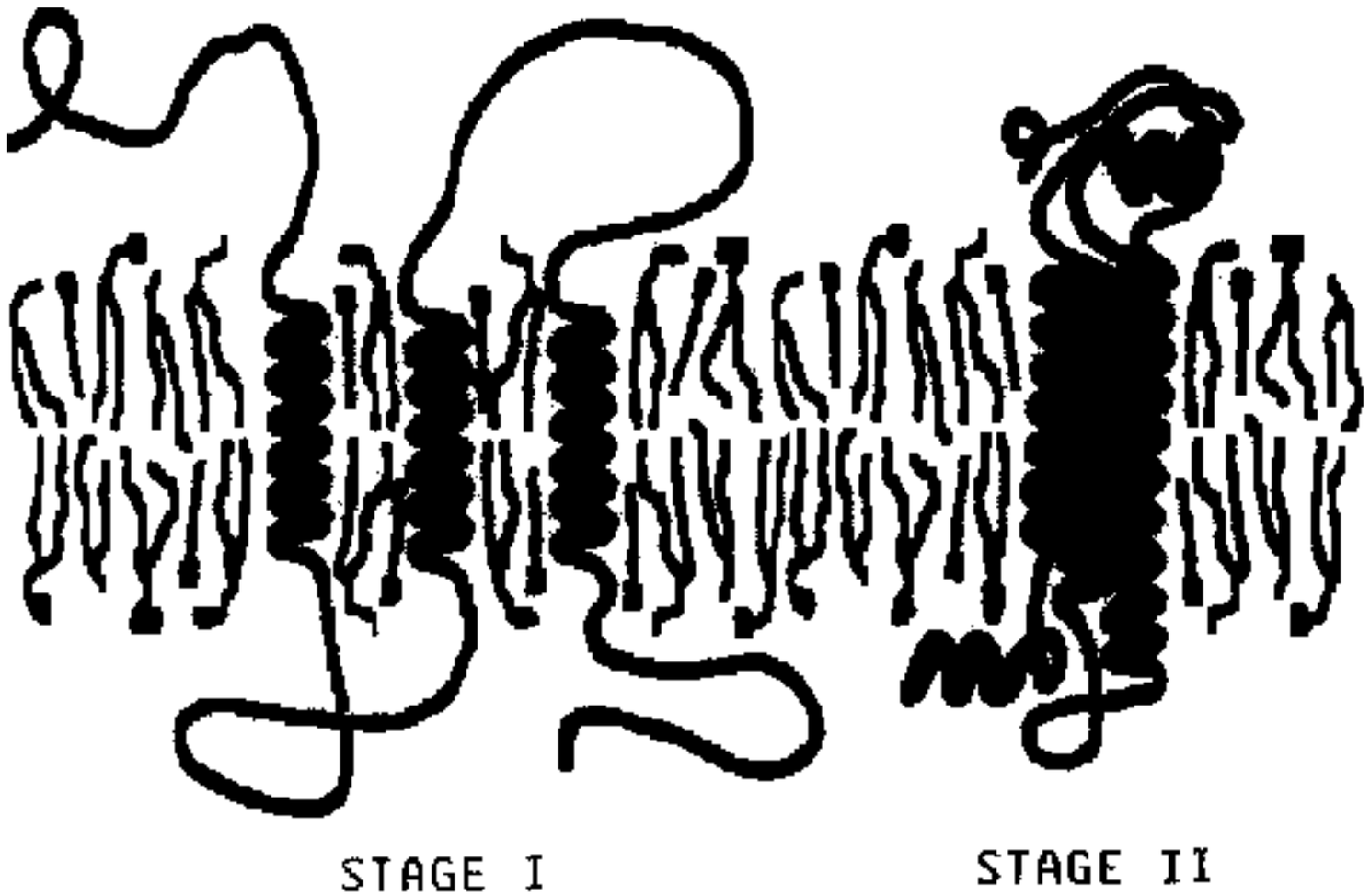

Popot JL, Engelman DM. Membrane protein folding and oligomerization: the two-stage model. Biochemistry. 1990 May 1;29(17):4031-7. doi: 10.1021/bi00469a001. PMID: 1694455.

The “two-stage” model is a bit more complex …

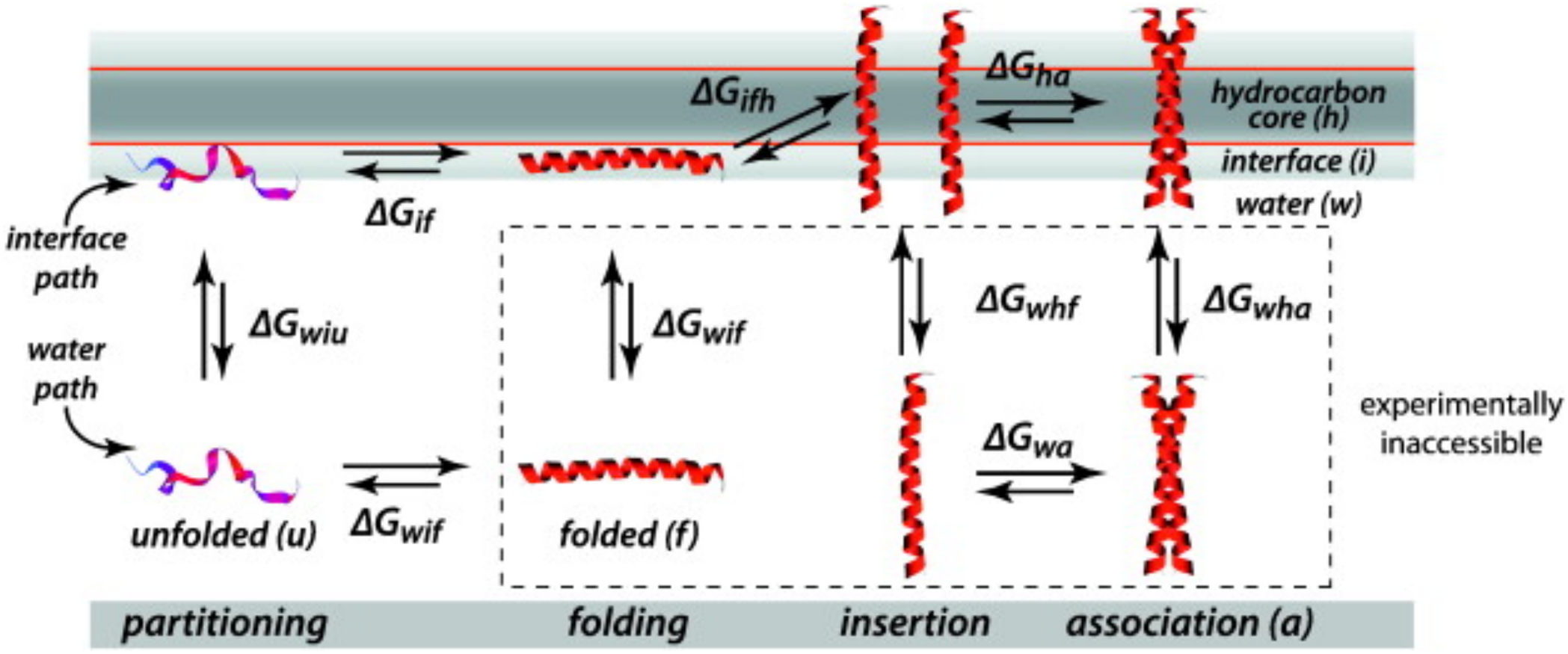

https://doi.org/10.1016/j.jmb.2014.09.014

The “two-stage” model is a bit more complex …

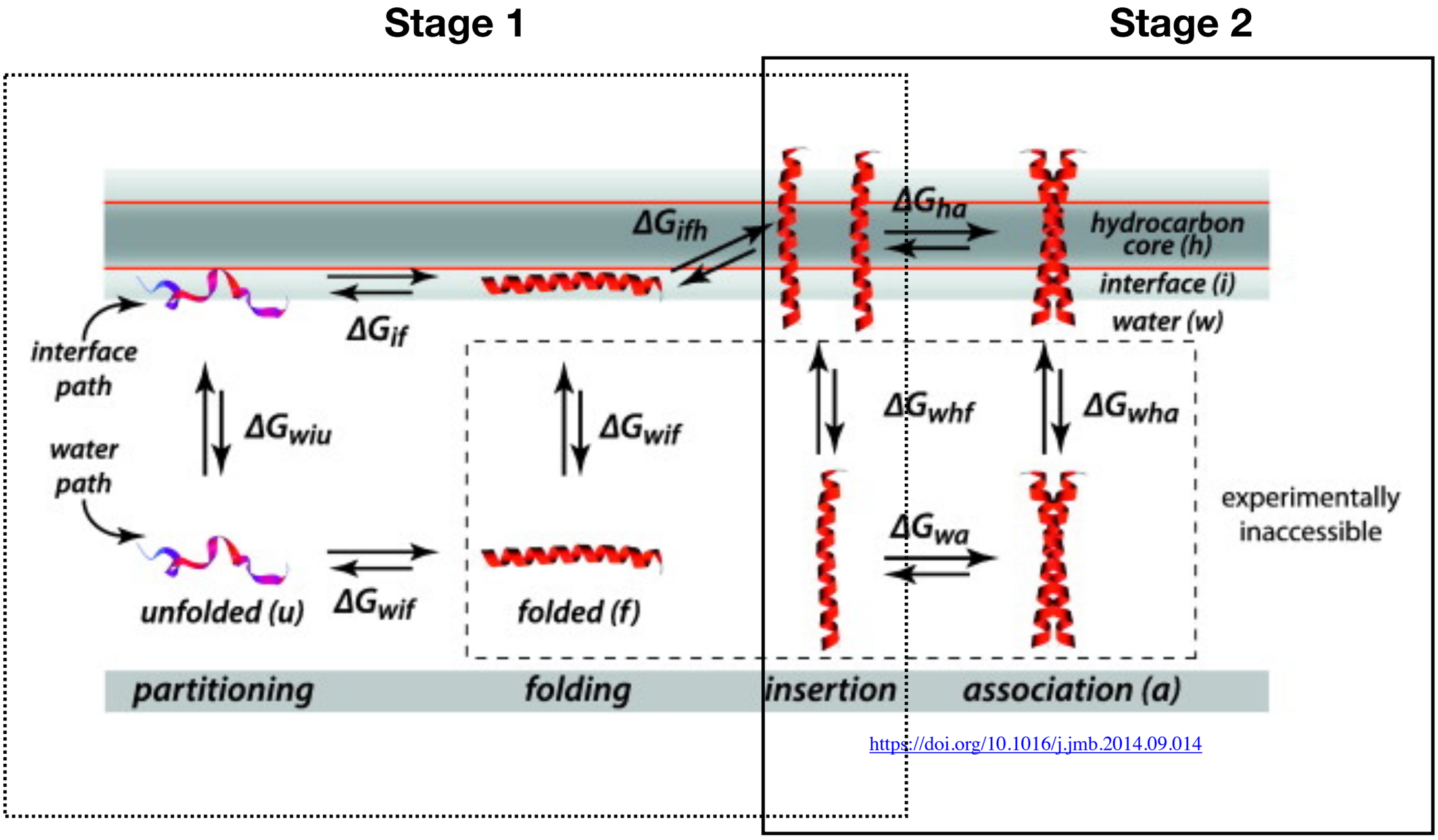

https://doi.org/10.1016/j.jmb.2014.09.014

Stage 1: Free energies of peptide partitioning

Figure 3.26 *Thermodynamic summary of TM helix stability. The free energy of insertion of a glycophorin transmembrane helix can be separated into two components: side chain and helical-backbone insertion free energies. The free energies of insertion are computed using the WW octanol scale (Figure 3.7). Although bulk octanol is not a perfect stand-in for the bilayer, the free energies for side chains and backbone are so large that errors in the difference free energies are unlikely to affect the general features of TM helix stability. As in many biochemical reactions, net free energies result from small differences between large opposing free energies. If the backbone of the helix is unfolded, the energetic cost of exposing non-H-bonded peptide bonds is so immense that the only TM structure possible is a helix. This observation explains why helices cannot be unfolded in calorimetric measurements (Figure 4.8).*

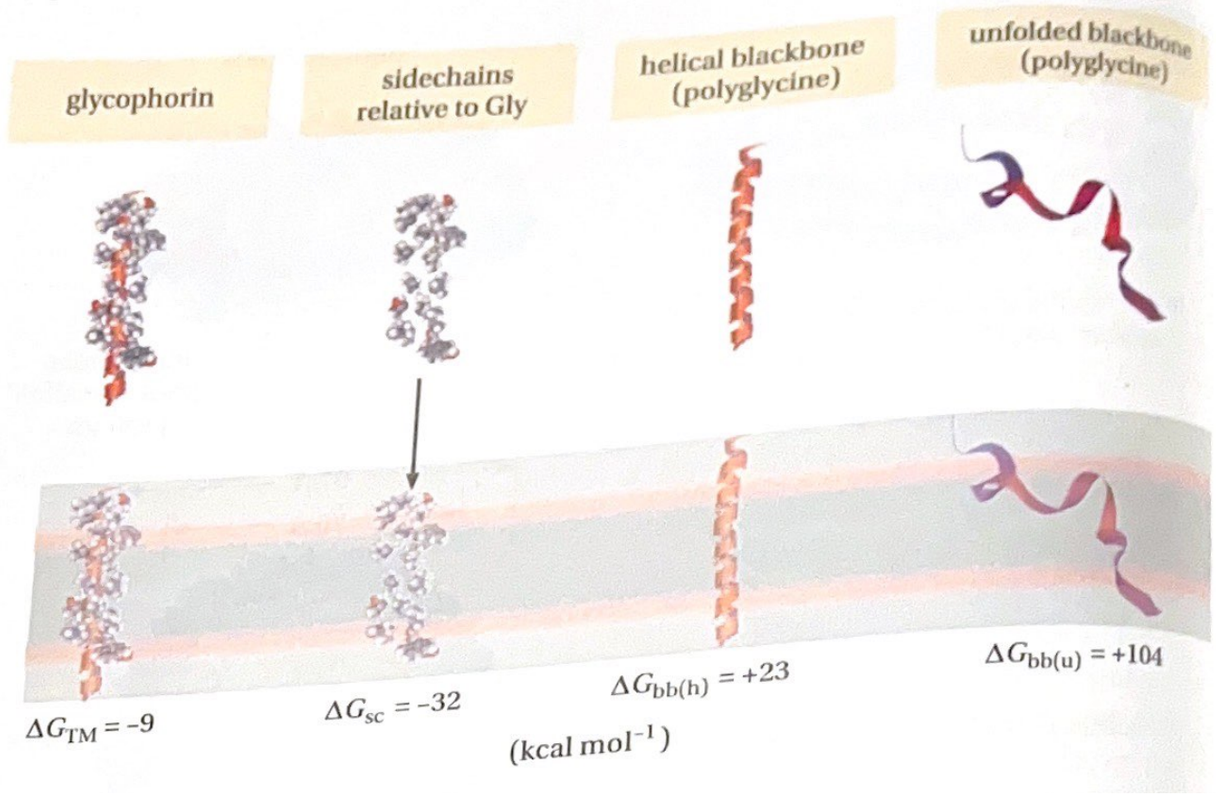

Stage 1: Measurements of equilibrium peptide partitioning

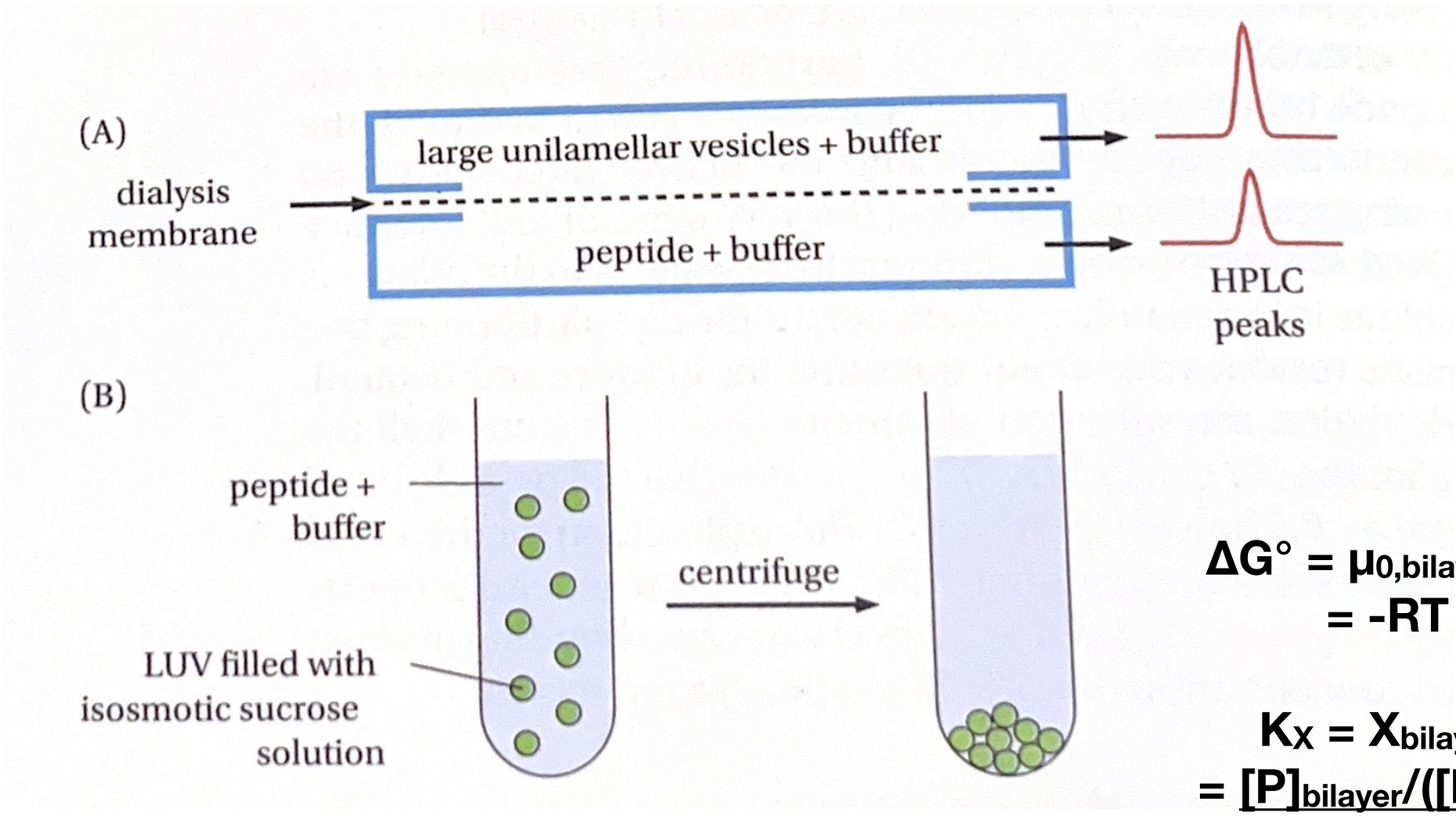

$$\Delta G^\circ = \mu_{0,bilayer} - \mu_{0,buffer} = -RT \ln K_X$$

$$K_X = X_{bilayer}/X_{buffer} = \frac{[P]_{bilayer}/([L]+[P]_{bilayer})}{[P]_{buffer}/([W]+[P]_{buffer})}$$

Stage 1: Peptide partitioning

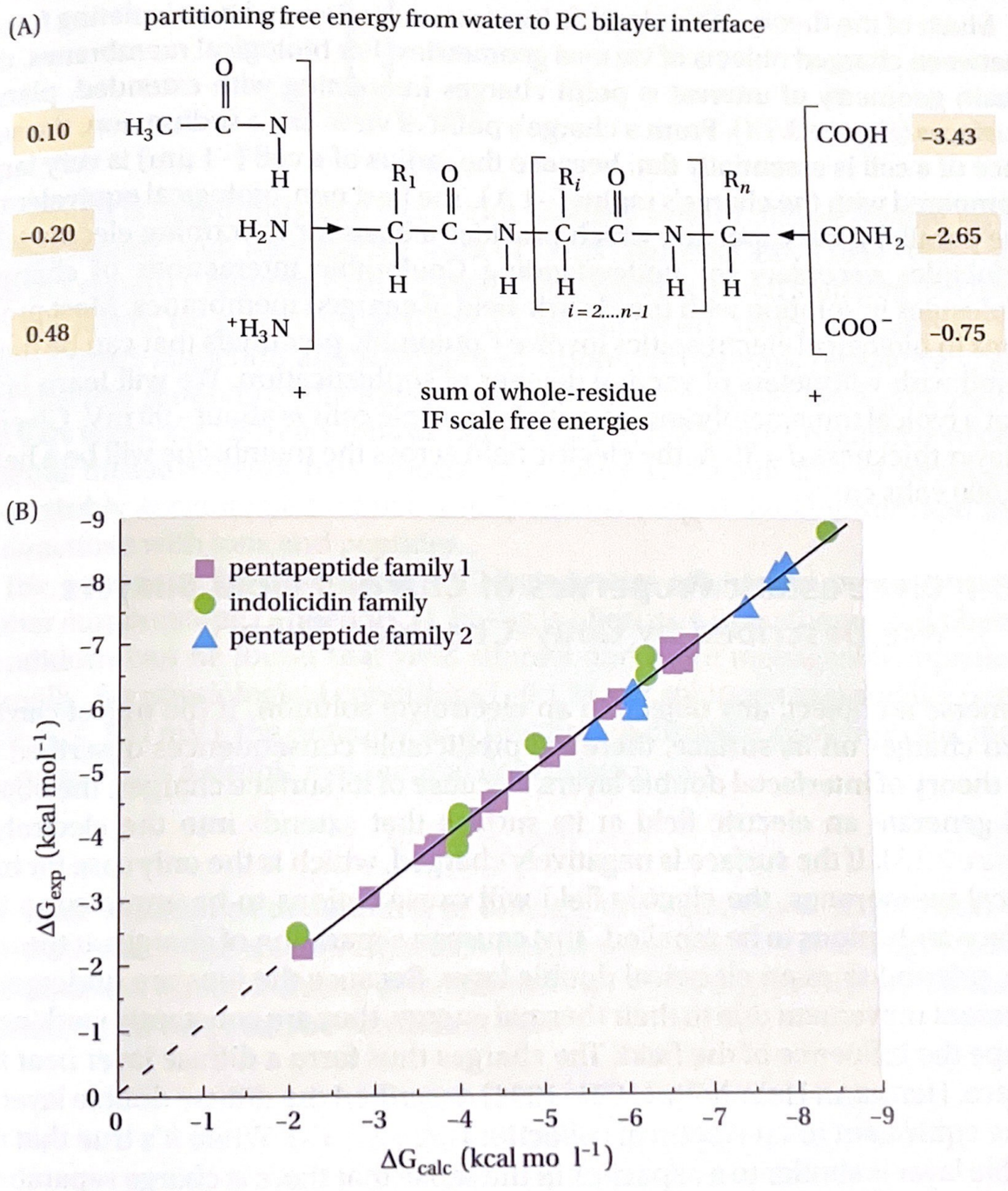

Figure 3.12 An experiment-based algorithm for predicting the partitioning of unfolded peptides into the POPC bilayer interface. (A) The algorithm accounts for the differing contributions of the peptide-terminating groups. Changes in the charge state of the C-terminus have a large effect on partitioning compared with the N-terminus. (B) A comparison of predicted (ΔG_{calc}) and measured (ΔG_{exp}) partitioning free energies. Within experimental error, the slope is 1 and the intercept is 0, meaning that the algorithm accurately predicts partitioning free energies for peptides that do not adopt regular secondary structure in water or bilayer. (From Hristova K, White SH [2005] *Biochemistry* 44:12614–12619, provided by author.)

Stage 2: Protein assembly inside the membrane

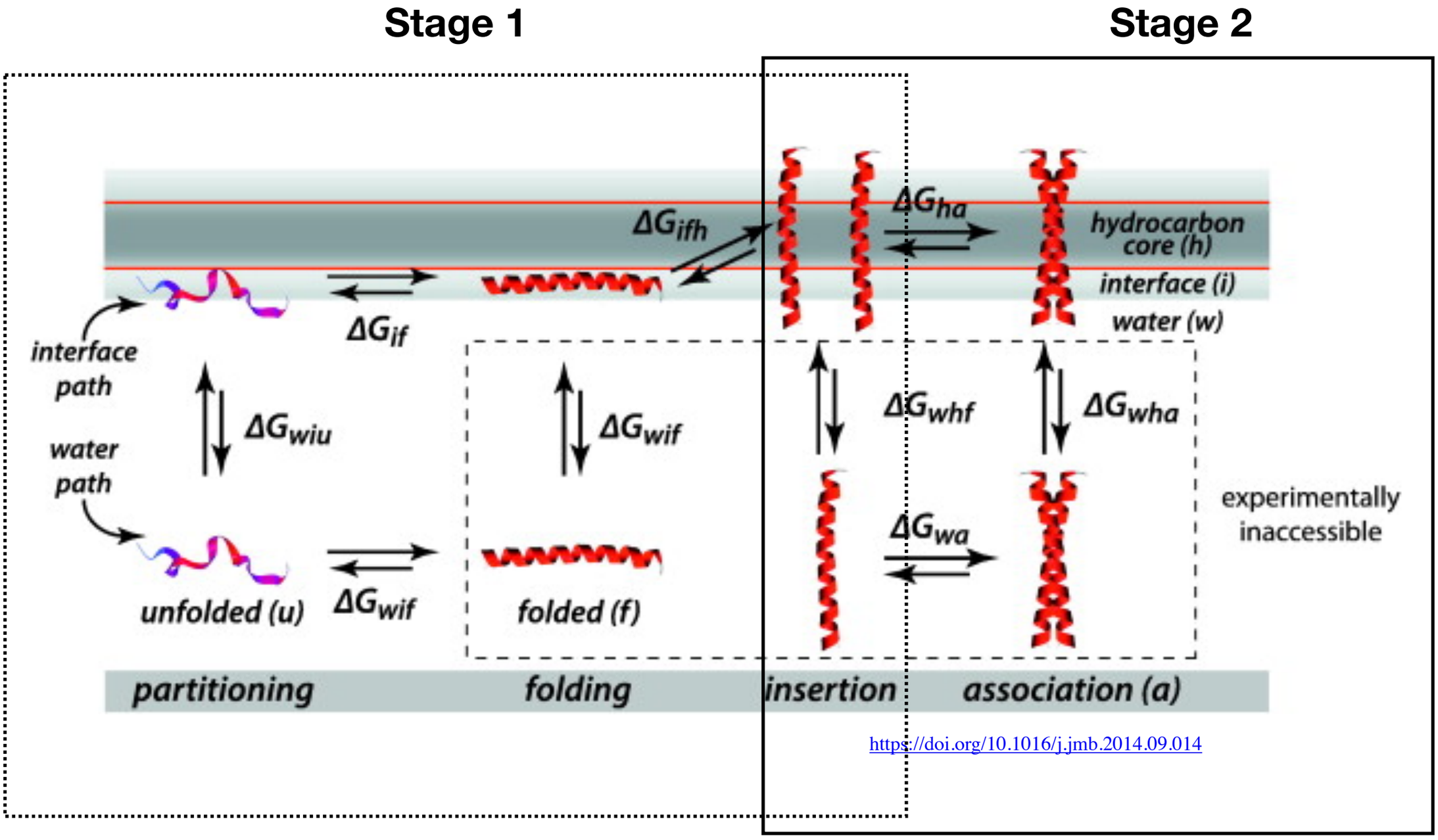

https://doi.org/10.1016/j.jmb.2014.09.014

Self-assembly of membrane proteins in membranes

The Torpedo electroplax membrane
50 Volts!

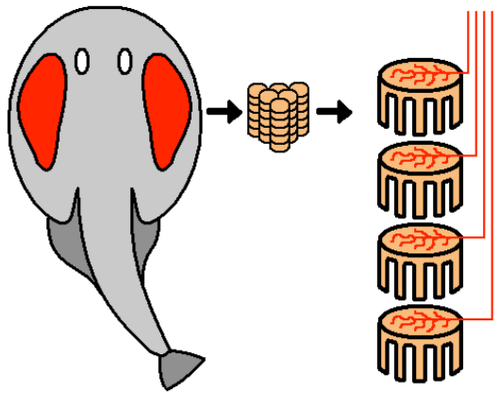

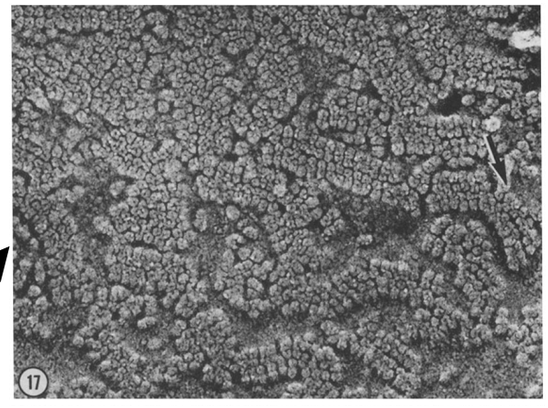

Heuser & Salpeter (JCB, 1979)

pure nicotinic acetylcholine receptor

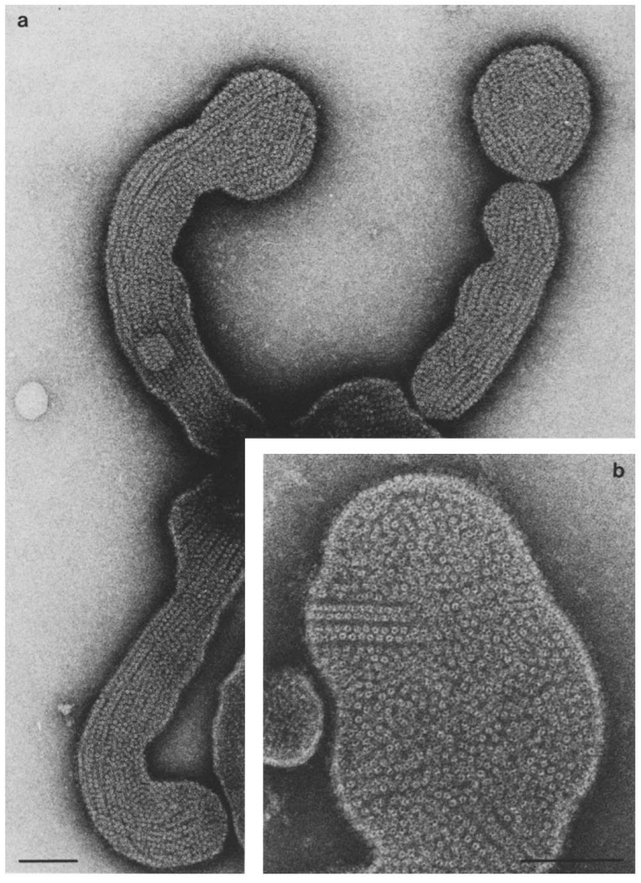

FIGURE 3 Vesicles with ribbons of paired receptors extending across their surfaces. The incubation conditions were 3 wk at 17°C. Bar, 0.1 μm. × 150,000. (*inset*) Bar, 0.1 μm. × 270,000.

Unwin (JCB, 1984)

500 Å

(*a*)

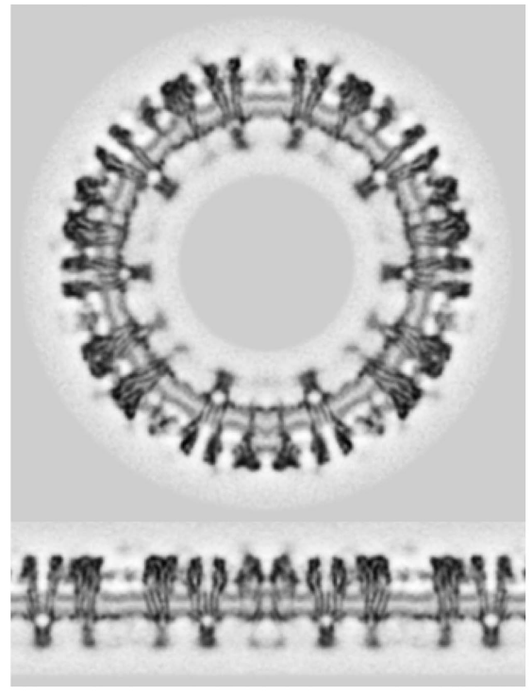

(*b*)

Unwin (IUCrJ, 2017)

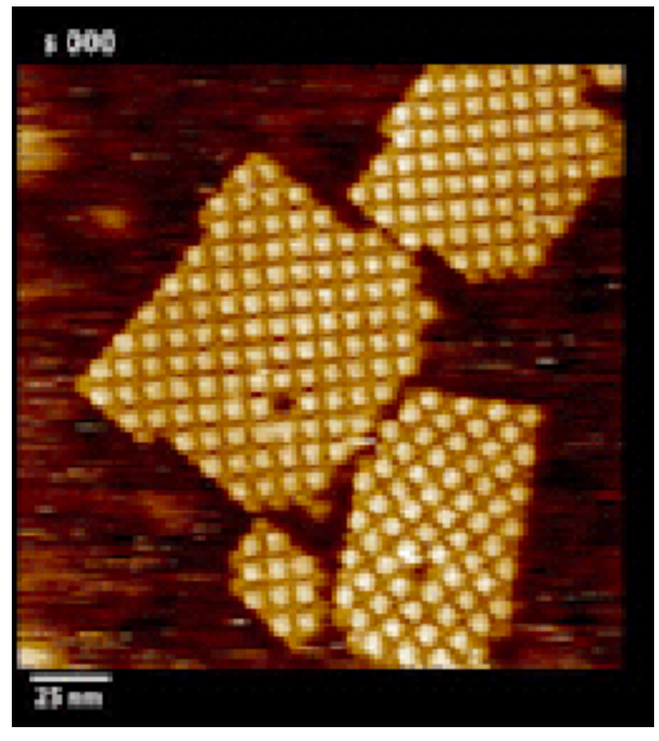

https://bio-afm-lab.com/hs-afm-movies/

Popot et al., 1987

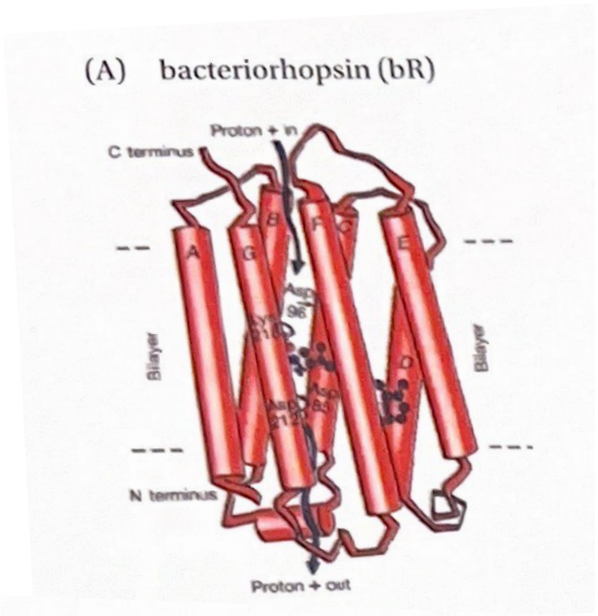

X-ray diffraction

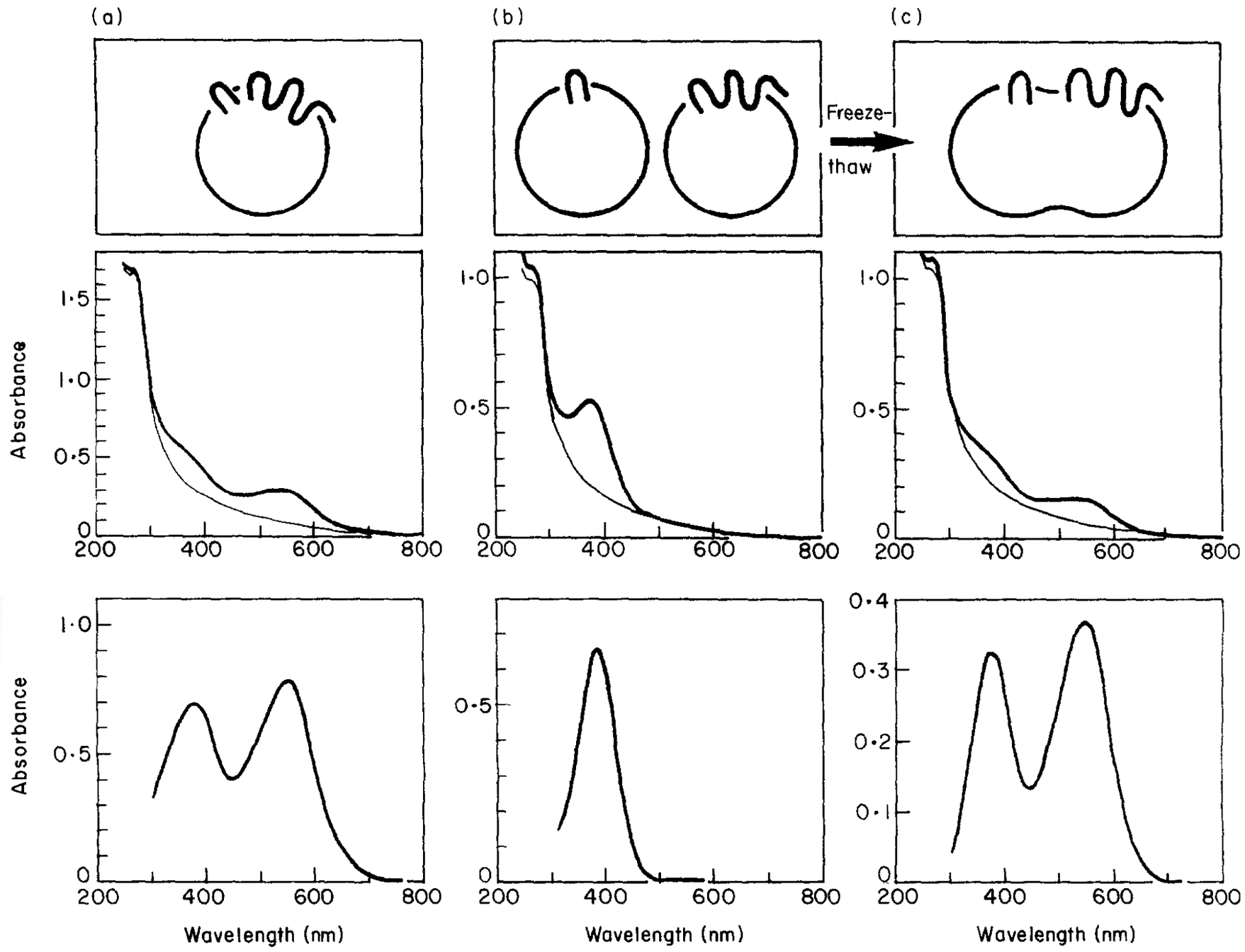

Figure 5. Regeneration of BR chromophore from fragments refolded either separately or simultaneously in the absence of retinal. Purified fragments in SDS buffer were mixed with *Halobacterium* lipids (lipid to protein ratio 10 : 1, w/w) in the absence of retinal and taurocholate and reconstituted by PDS precipitation as described in Materials and Methods. Following dialysis, the vesicle suspensions were clarified by a brief sonication. (a) C-1 and C-2 in SDS buffer were mixed prior to PDS precipitation and simultaneously refolded in the same vesicles (top panel). Absorption spectra were recorded before (thin line) and after (thick line) addition of excess retinal (middle panel). Bottom: difference spectrum. (b) C-1 and C-2 were reconstituted into separate vesicles (top panel). The vesicles were mixed (equimolar ratio of the fragments) and absorption spectra recorded before (thin line) and after (thick line) addition of excess retinal (middle panel). Bottom: difference spectrum. (c) C-1 and C-2 were reconstituted into separate vesicles. The vesicles were mixed (equimolar ratio of the fragments) and freeze–thawed (top panel) in the absence (thin line) or presence (thick line) of excess retinal (middle panel). Absorption spectra were recorded after clarification by brief sonication. The identical result was obtained if retinal was added after freeze–thawing. Bottom: difference spectrum.

In-membrane oligomeric assembly of membrane transporters & ion channels (e.g., CLC)

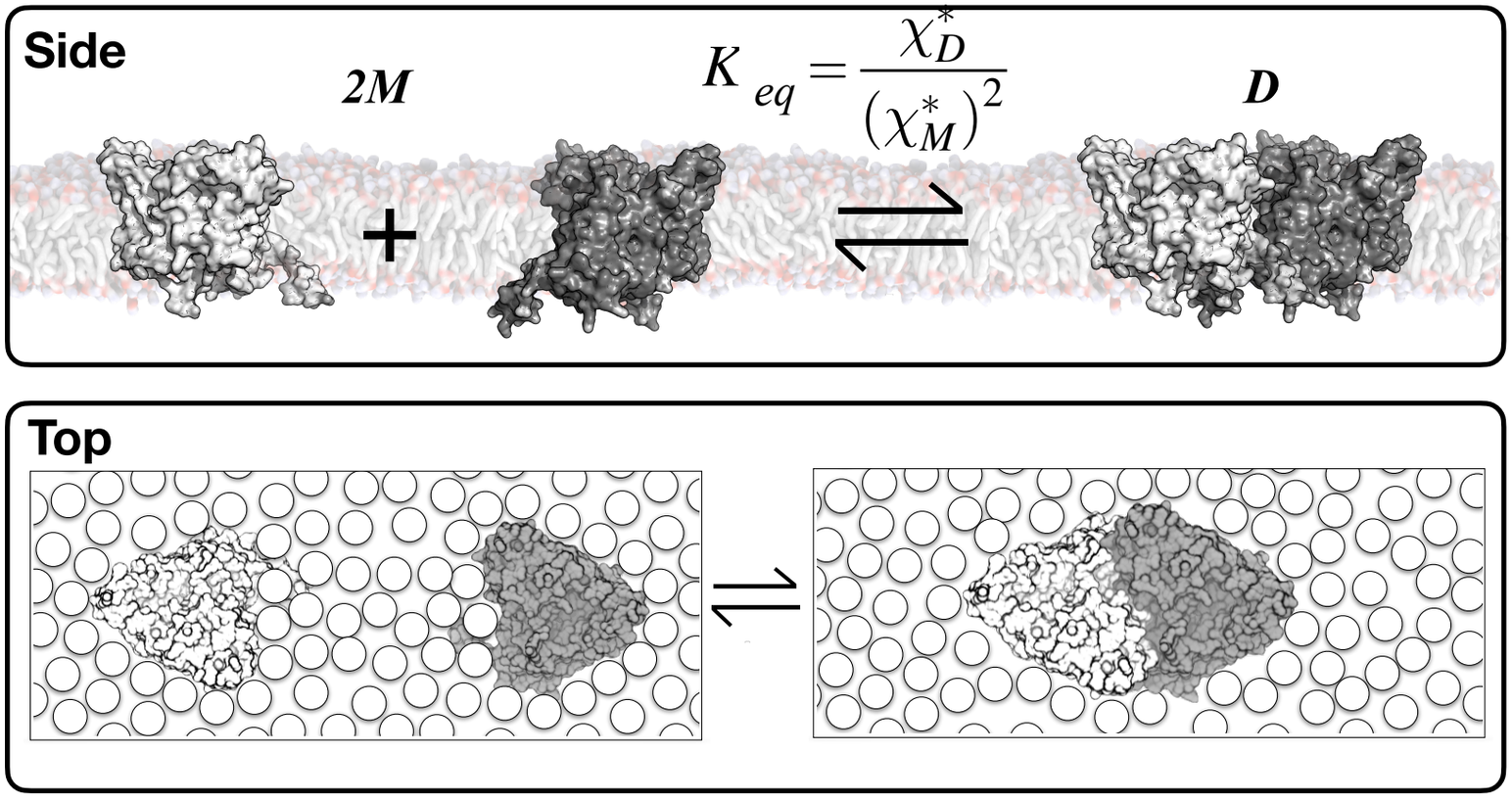

Measuring membrane protein association equilibrium in membranes by single molecule subunit capture

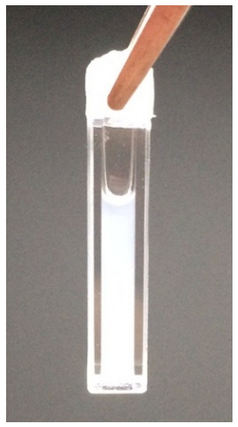

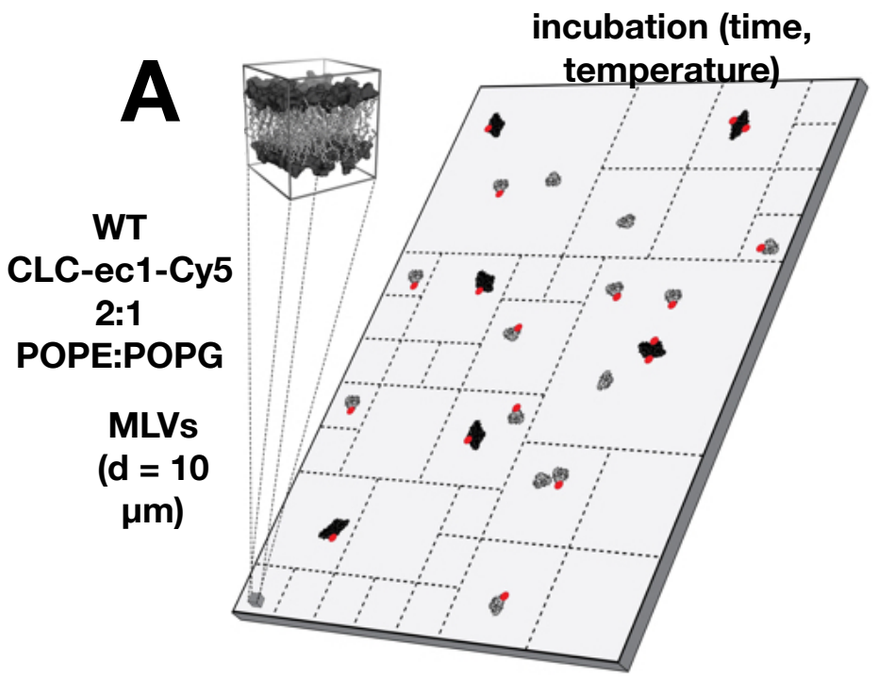

Chadda & Robertson, MIE 2016

Dimerization isotherms of CLC-ec1 in membranes

$$F_{Dimer} = \frac{1 + 4\chi^* K_{eq} - \sqrt{1 + 8\chi^* K_{eq}}}{4\chi^* K_{eq}}$$

$$\Delta G° = -RT\, ln(K_{eq} \cdot \chi^\circ)$$

$$\chi^\circ = 1\,\frac{subunit}{lipid}$$

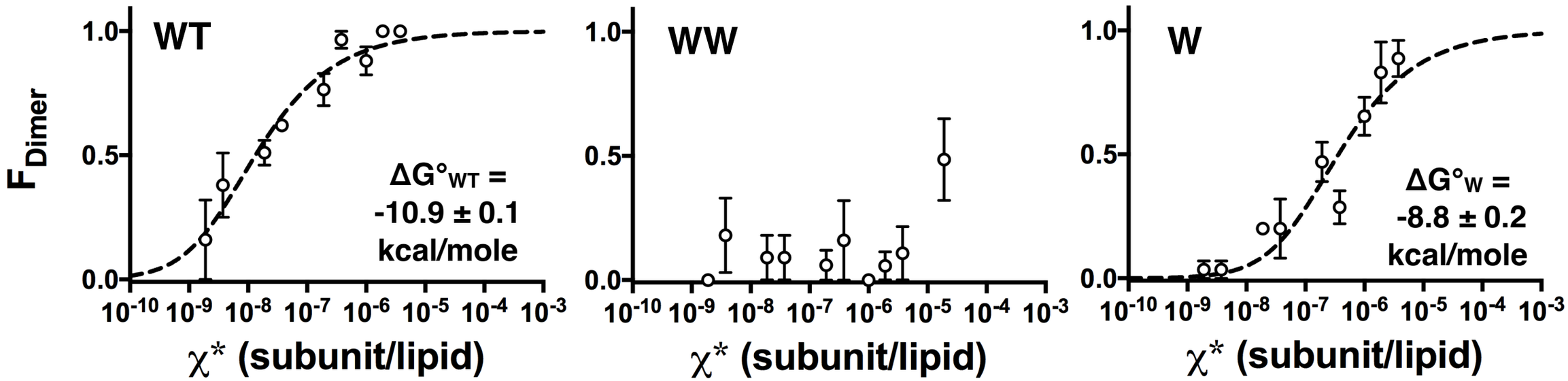

Chadda, Krishnamani, Mersch, Wong, Brimberry, Chadda, Kolmakova-Partensky, Friedman, Gelles & Robertson, eLIFE 2016 Chadda, Cliff, Brimberry & Robertson, JGP 2018

Steric trapping for kinetically limited reactions

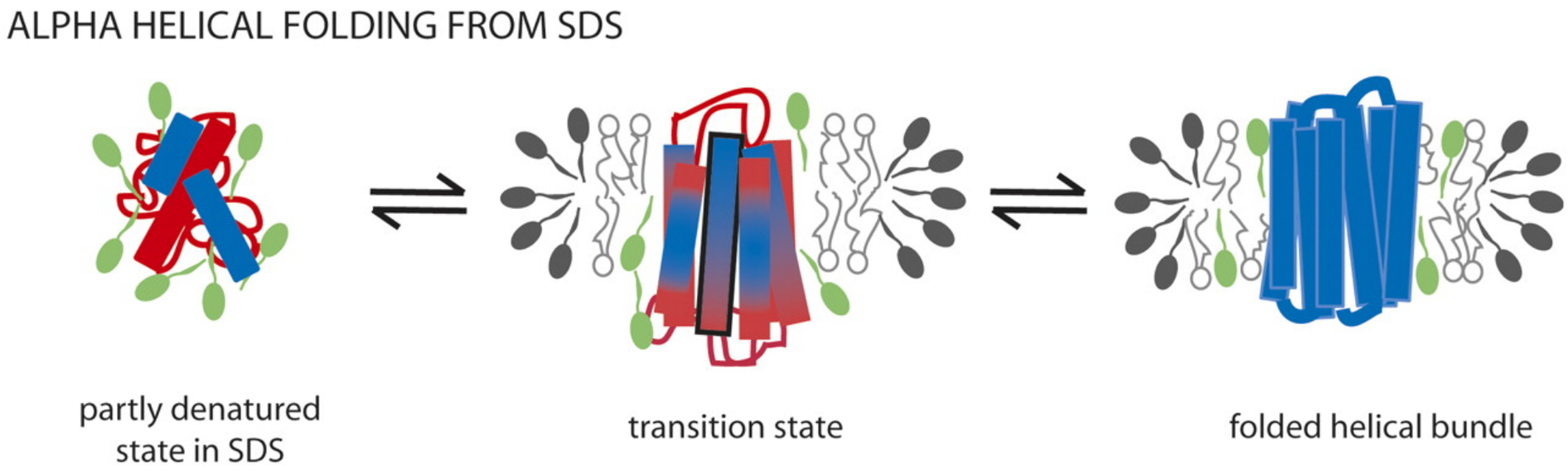

Steric-trapping studies folding in the native state

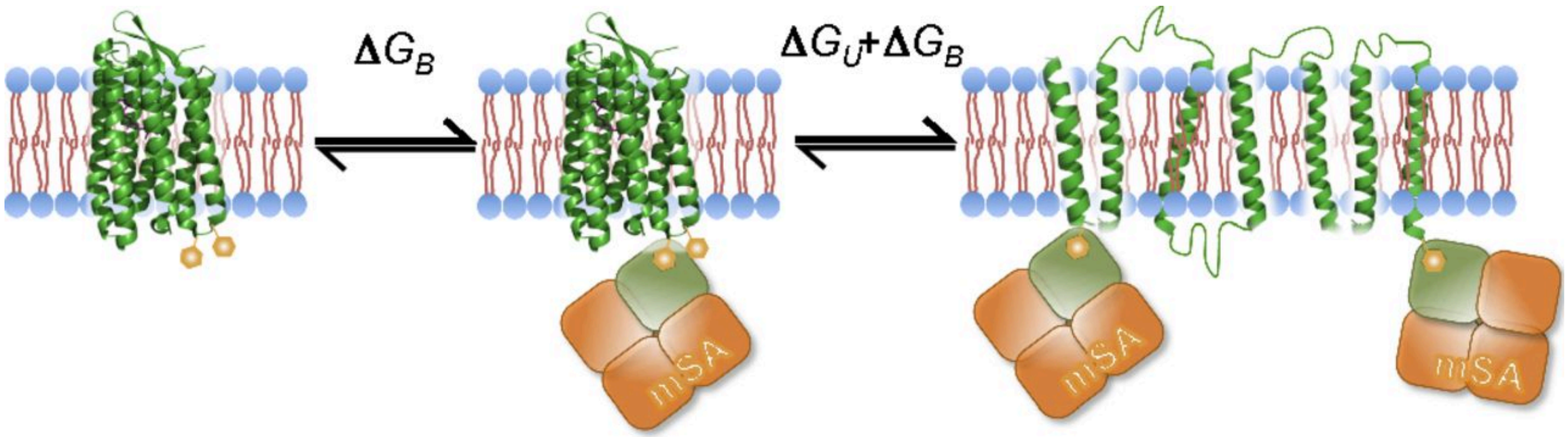

Single-molecule force microscopy methods

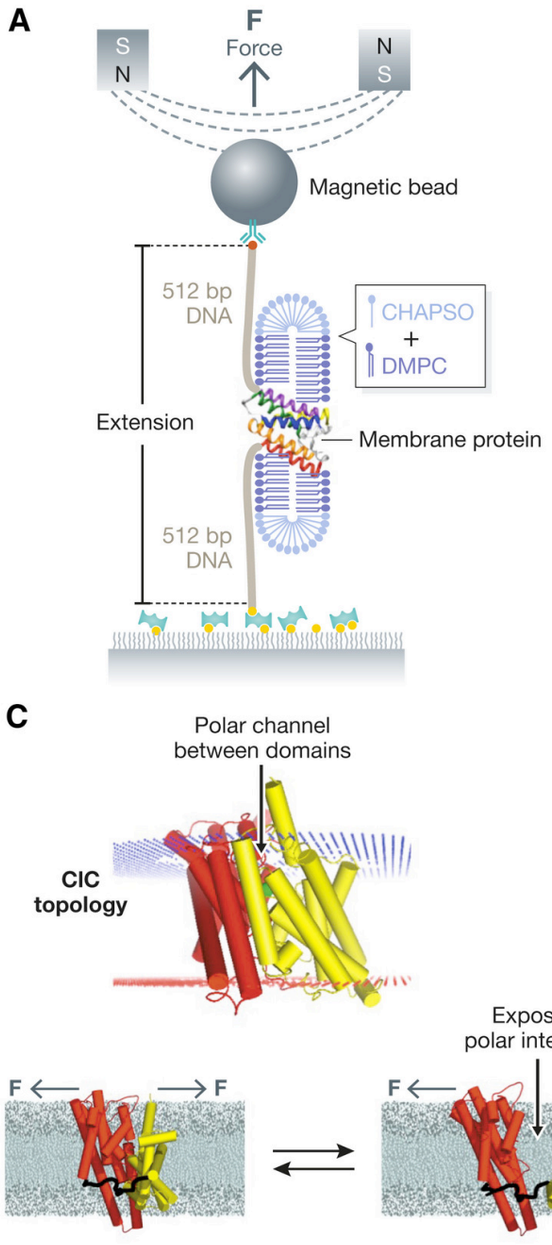

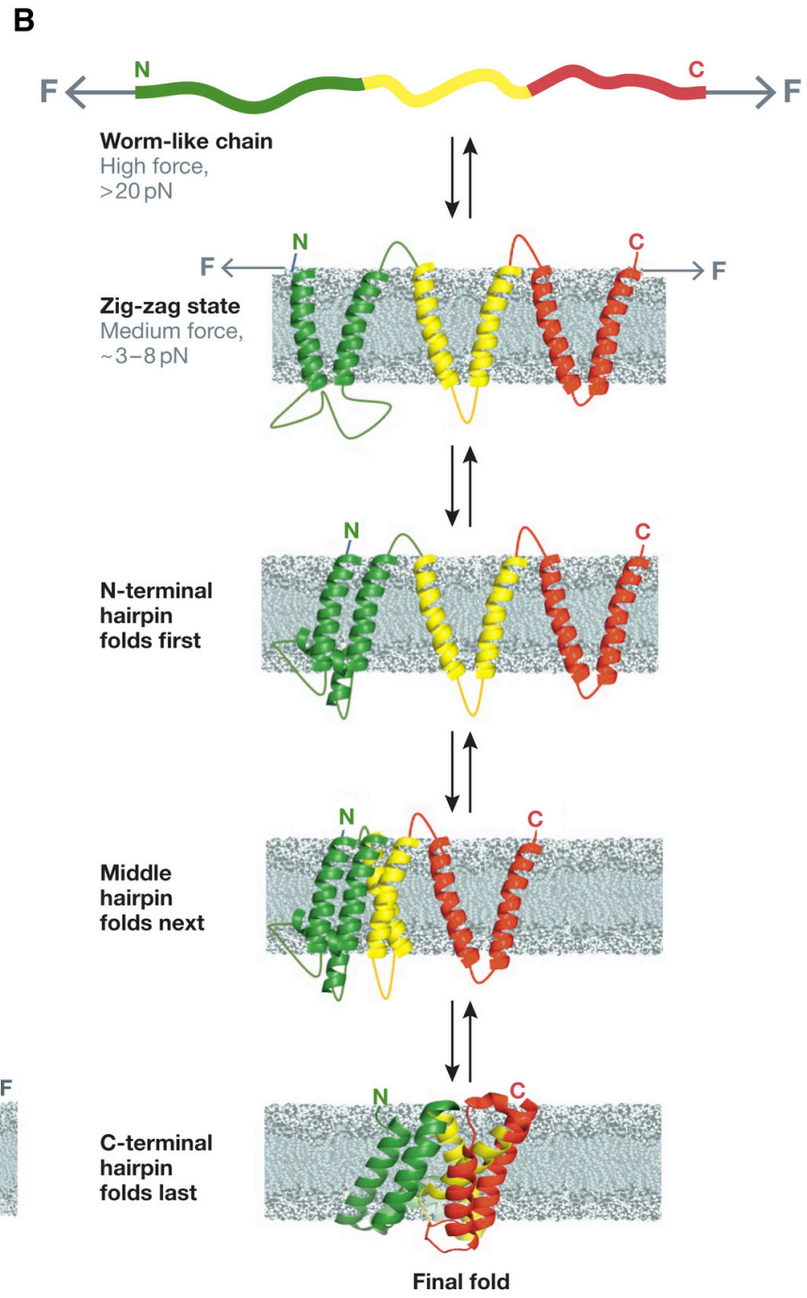

Gramicidin dimerization is sensitive to membrane properties

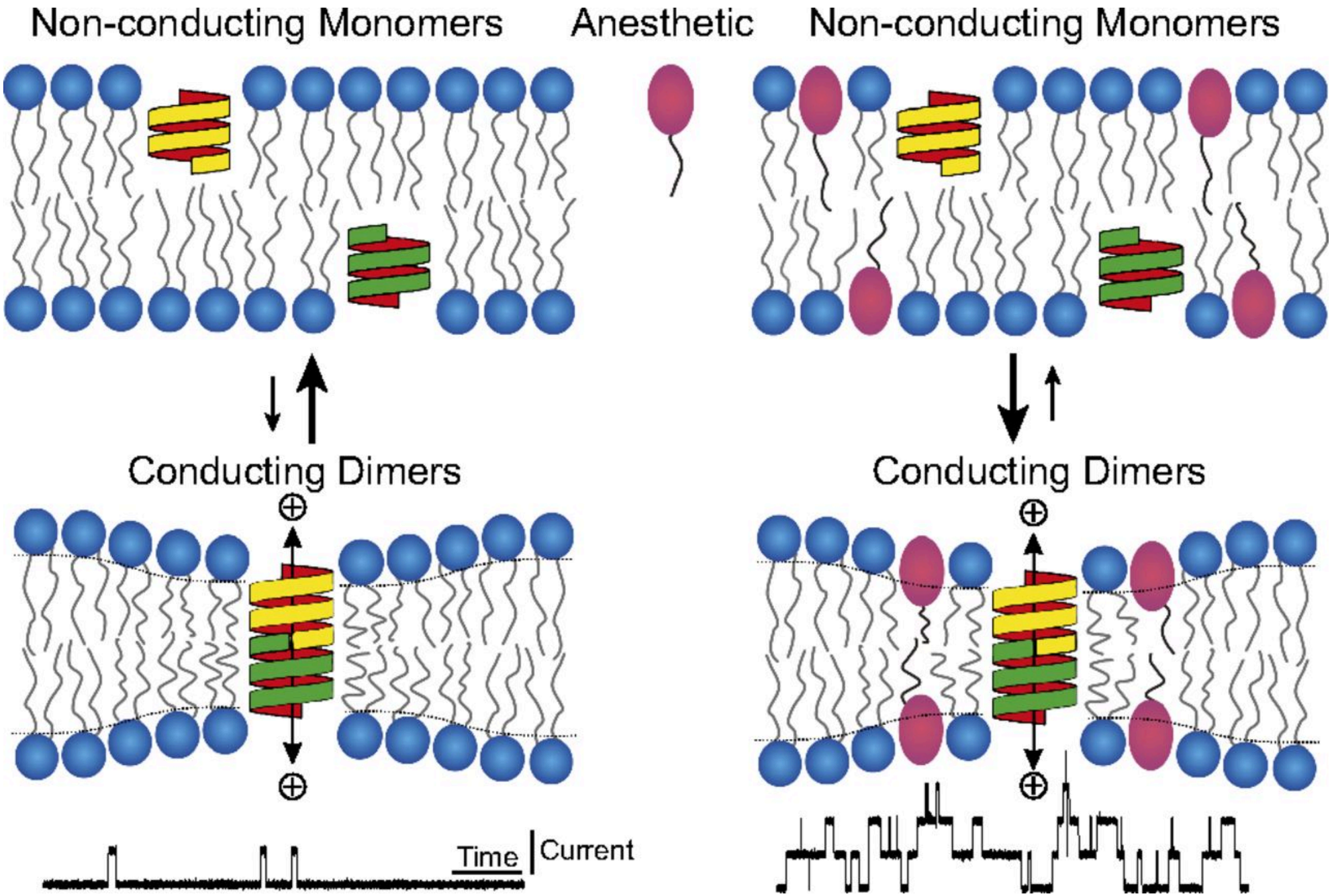

https://doi.org/10.1073/pnas.1611717114

What are the driving forces for membrane protein stability

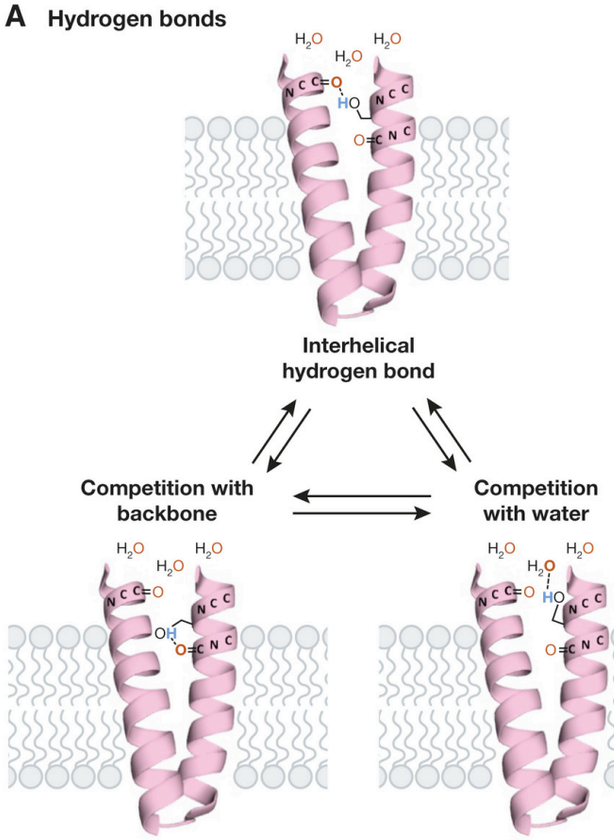

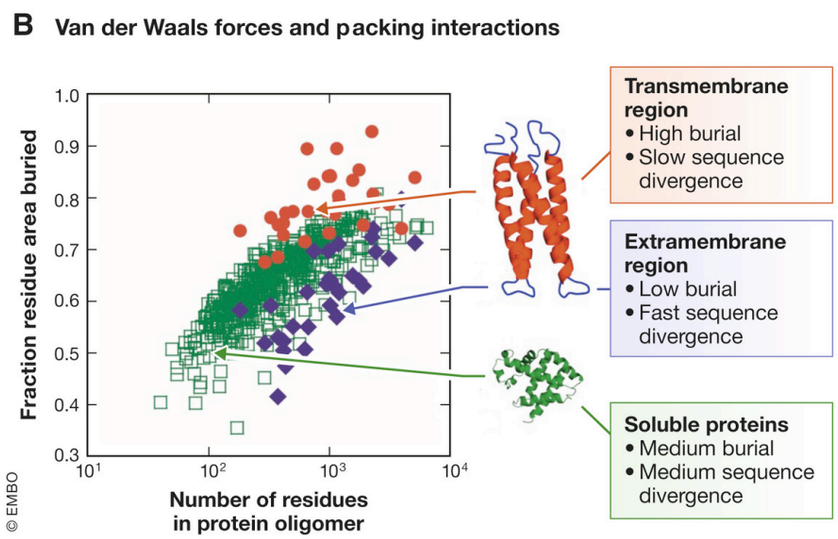

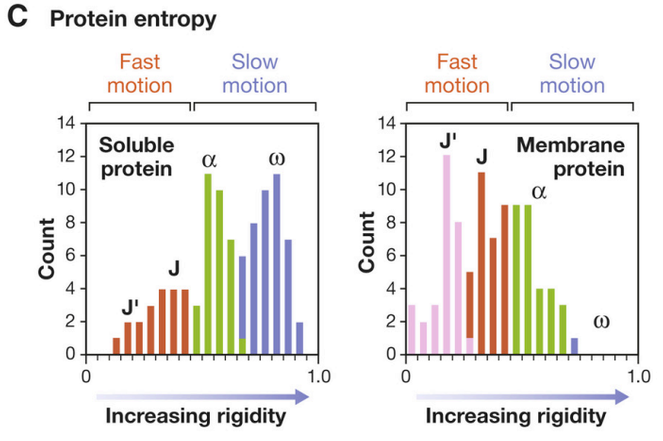

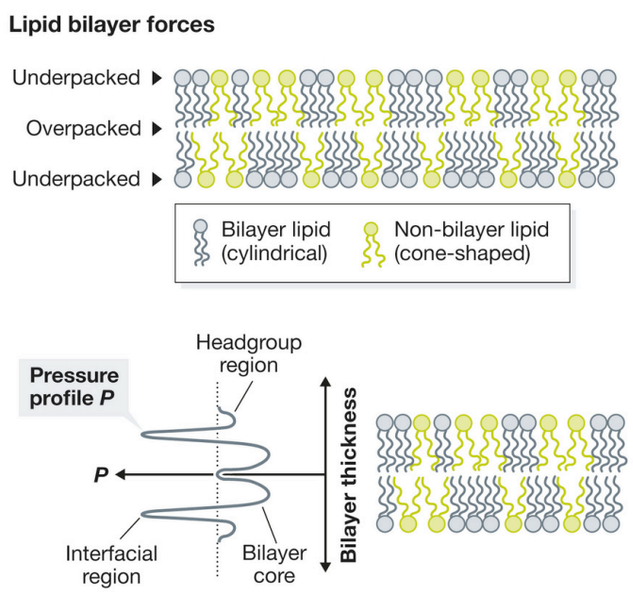

CLC dimers driven by burial of membrane defects (mimicking the hydrophobic effect)

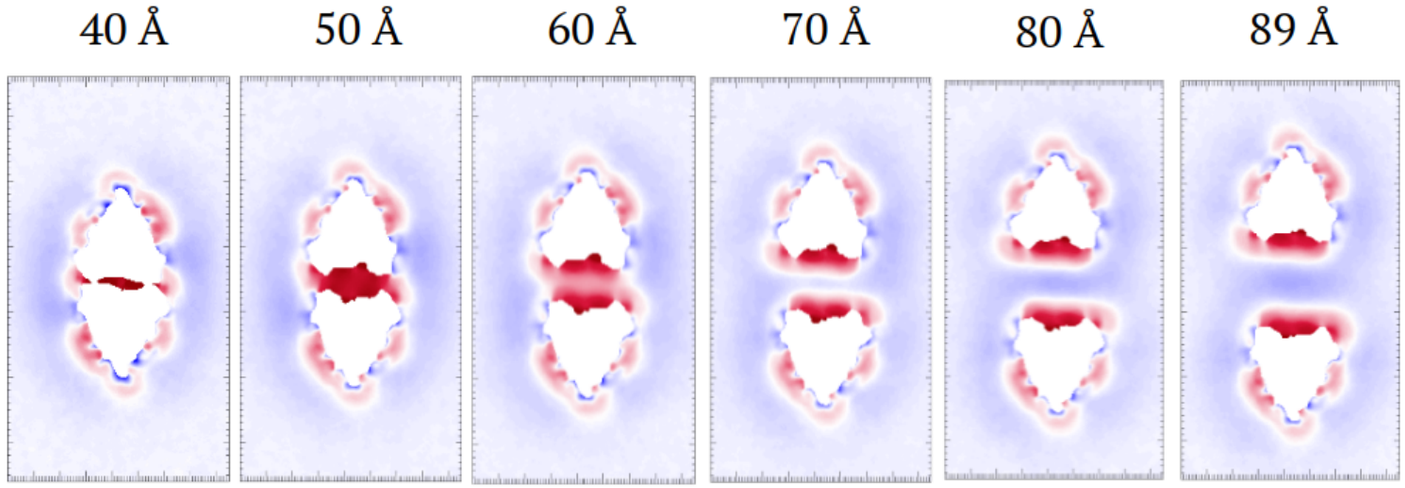

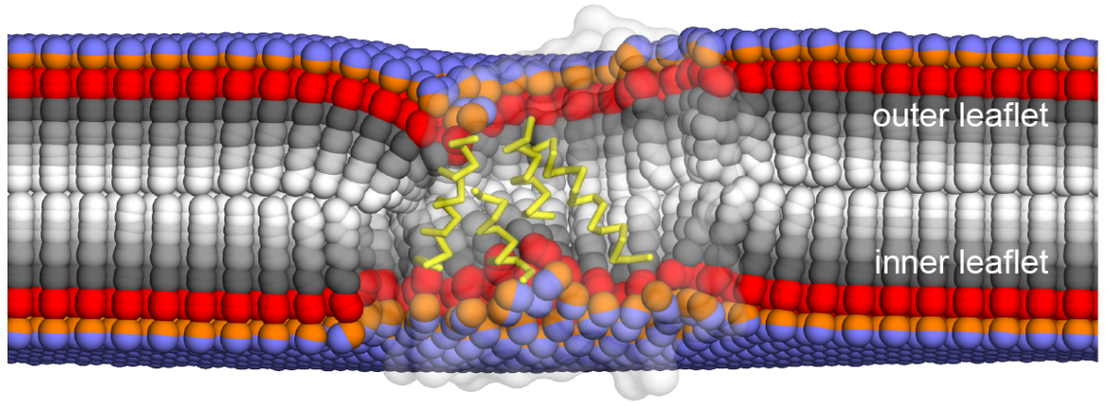

time-averaged lipid structures

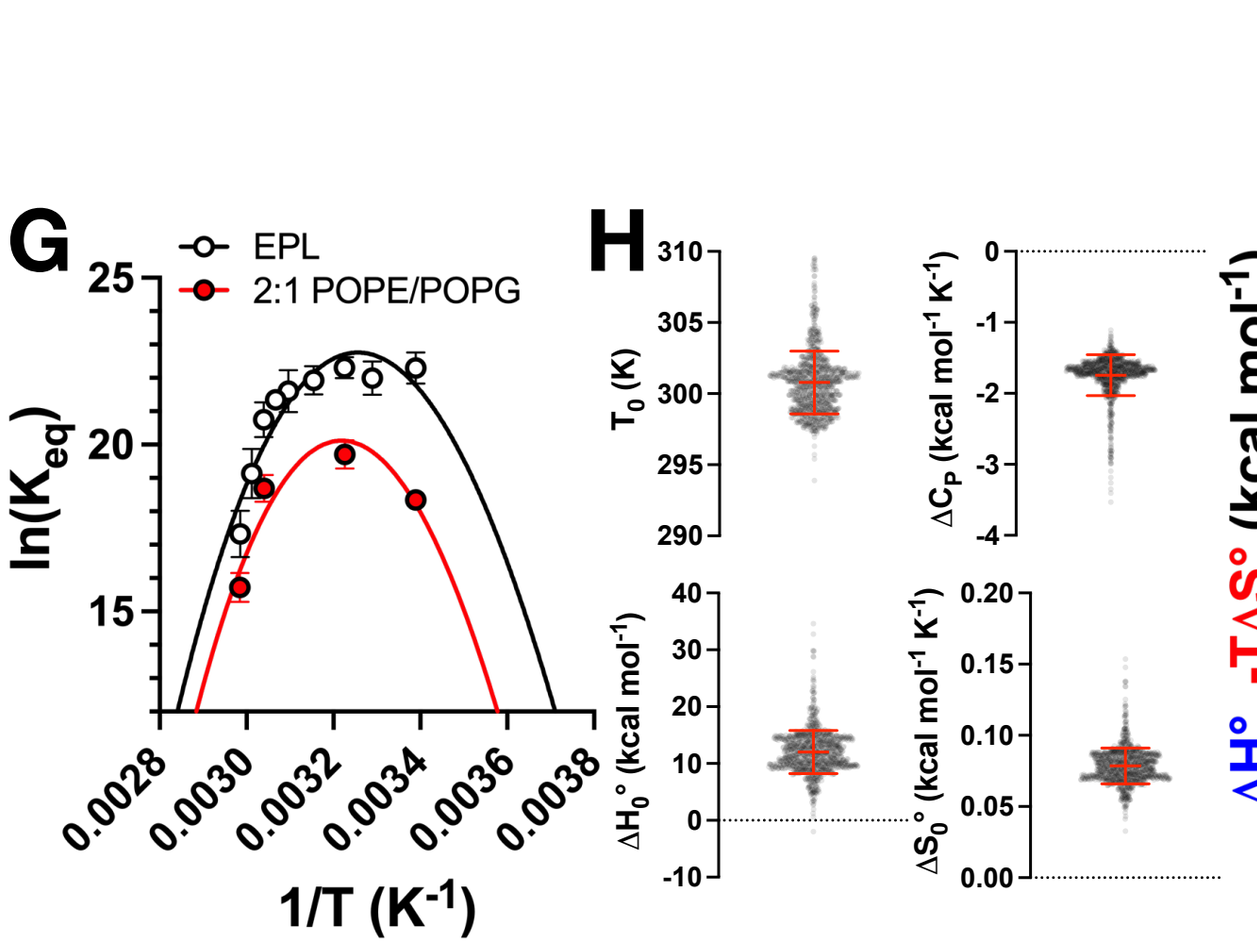

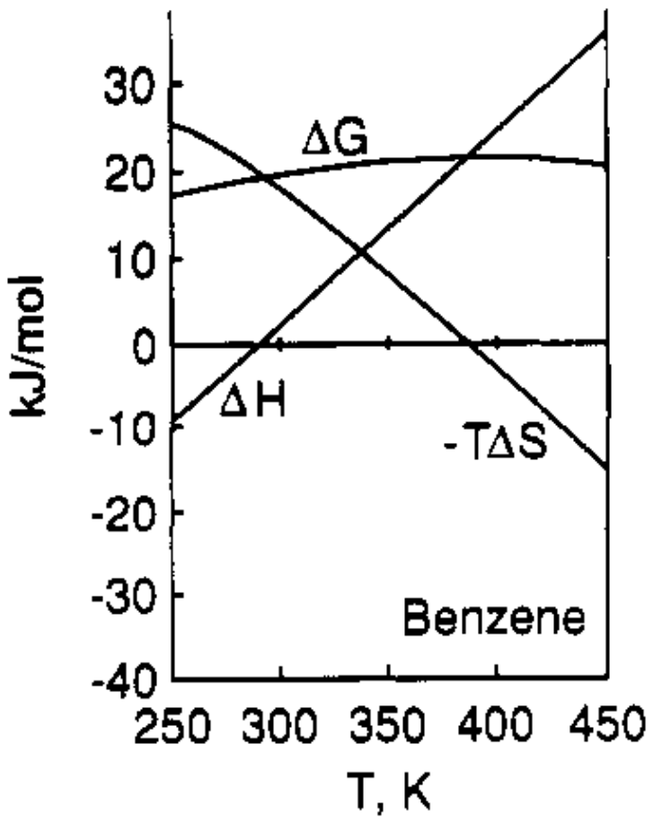

Non-linear van't Hoff of benzene partitioning into water

From Dill 1990, adapted from Privalov & Gill 1988.

What is the role of lipids in protein reactions? Solvent or ligands?

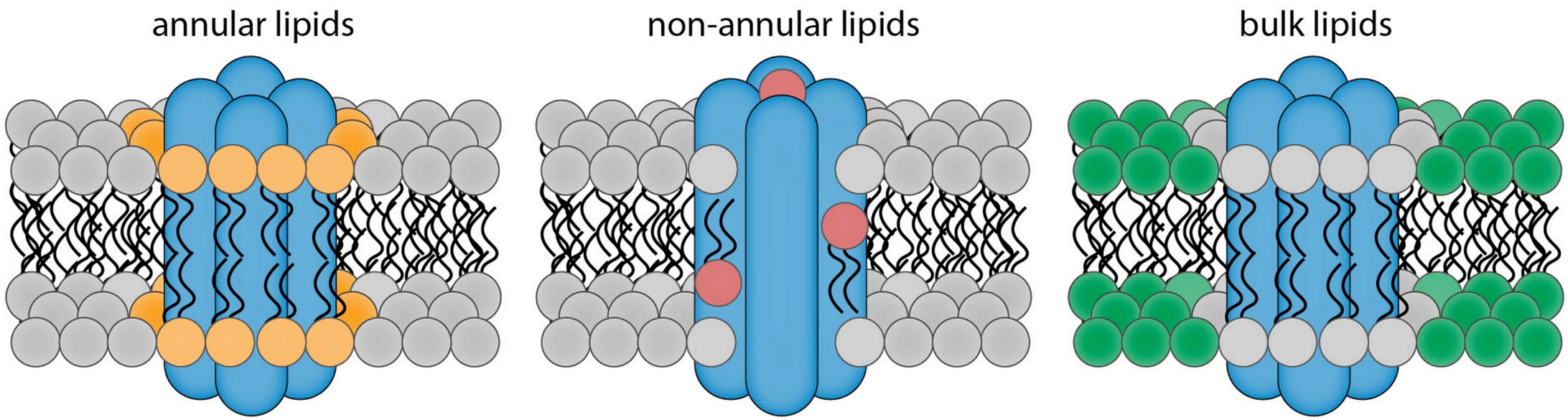

- **ESR reports lipid exchange between annular lipids as ~ 10^7 s^{-1}**
- **Lipid exchange in bulk ~ 10^8 s^{-1}**
- **Intrinsically different membrane environment around a protein**
- **Not necessarily binding**

Frick M, Schmidt C. Mass spectrometry-A versatile tool for characterising the lipid environment of membrane protein assemblies. Chem Phys Lipids. 2019 Jul;221:145-157. doi: 10.1016/j.chemphyslip.2019.04.001. Epub 2019 Apr 3. PMID: 30953608.

Lipids link to equilibrium by co-solvent effects

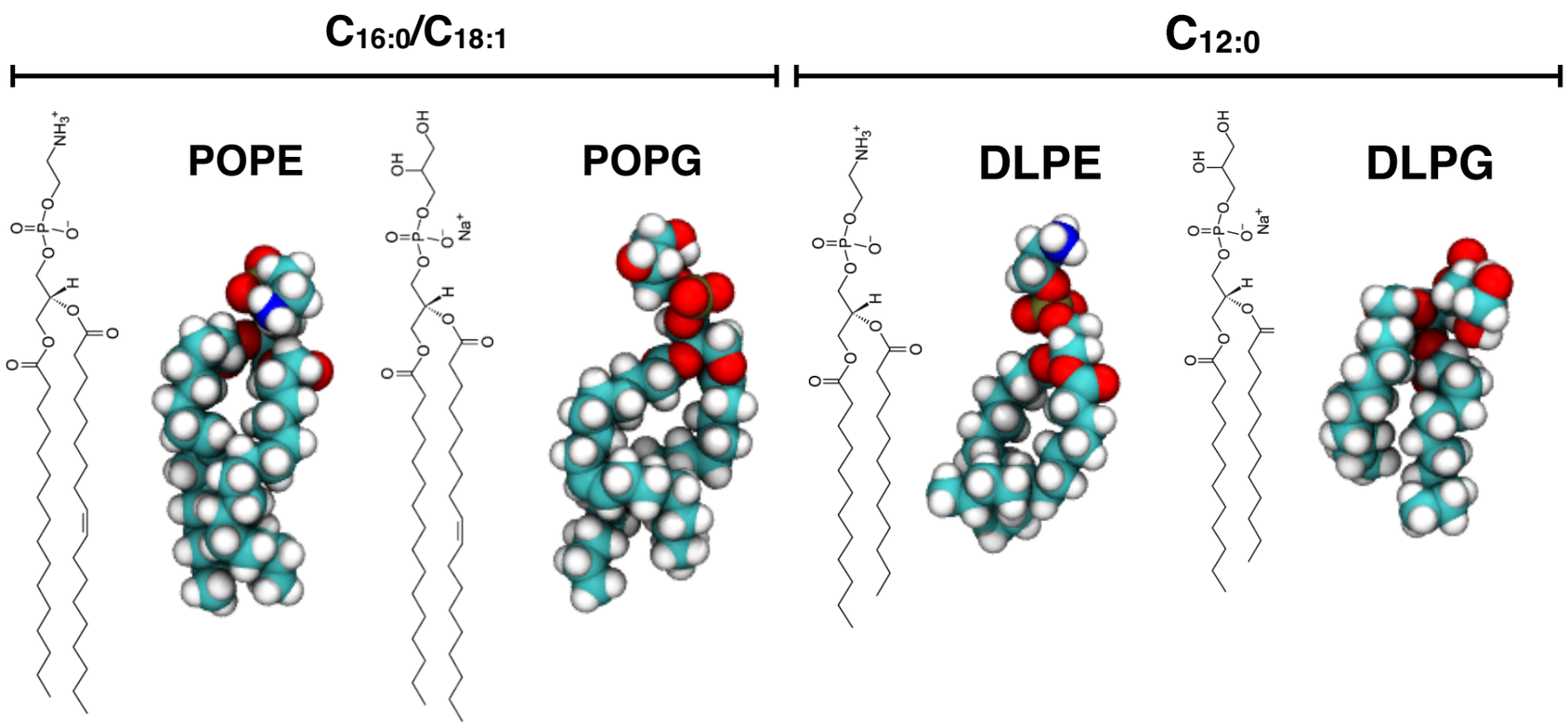

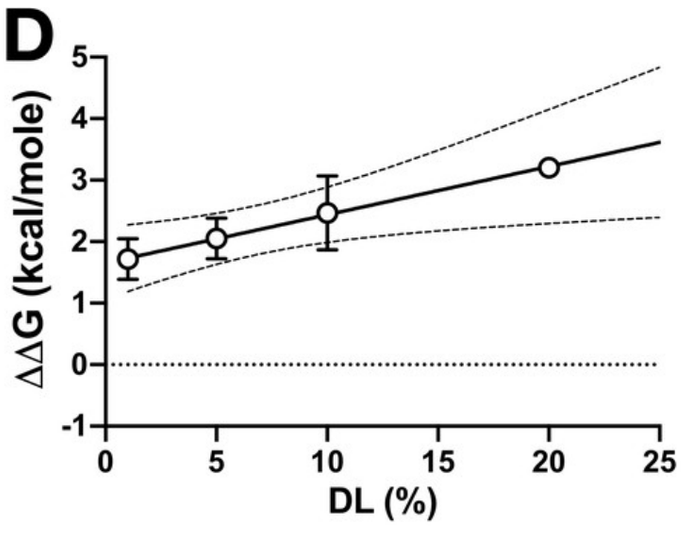

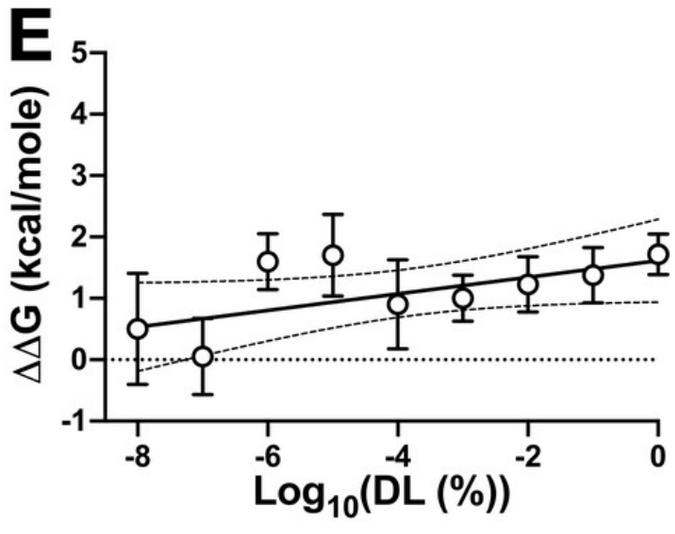

ΔΔG ∝ log(DL) → preferential solvation

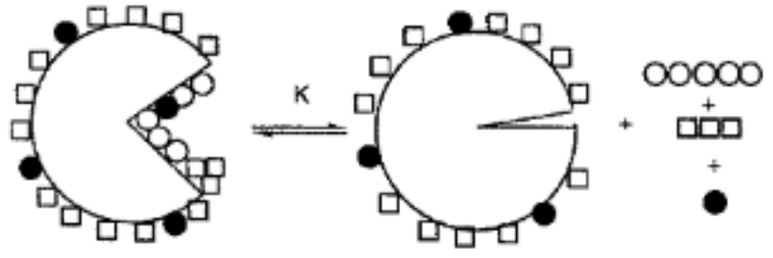

Timasheff, 2002

Chadda, Bernhardt, Kelley, Teixeira, Griffith, Gil-Ley, Ozturk, Hughes, Forsythe, Krishnamani, Faraldo-Gómez* & Robertson*, eLife 2021

Soluble vs. Membrane Protein Folding

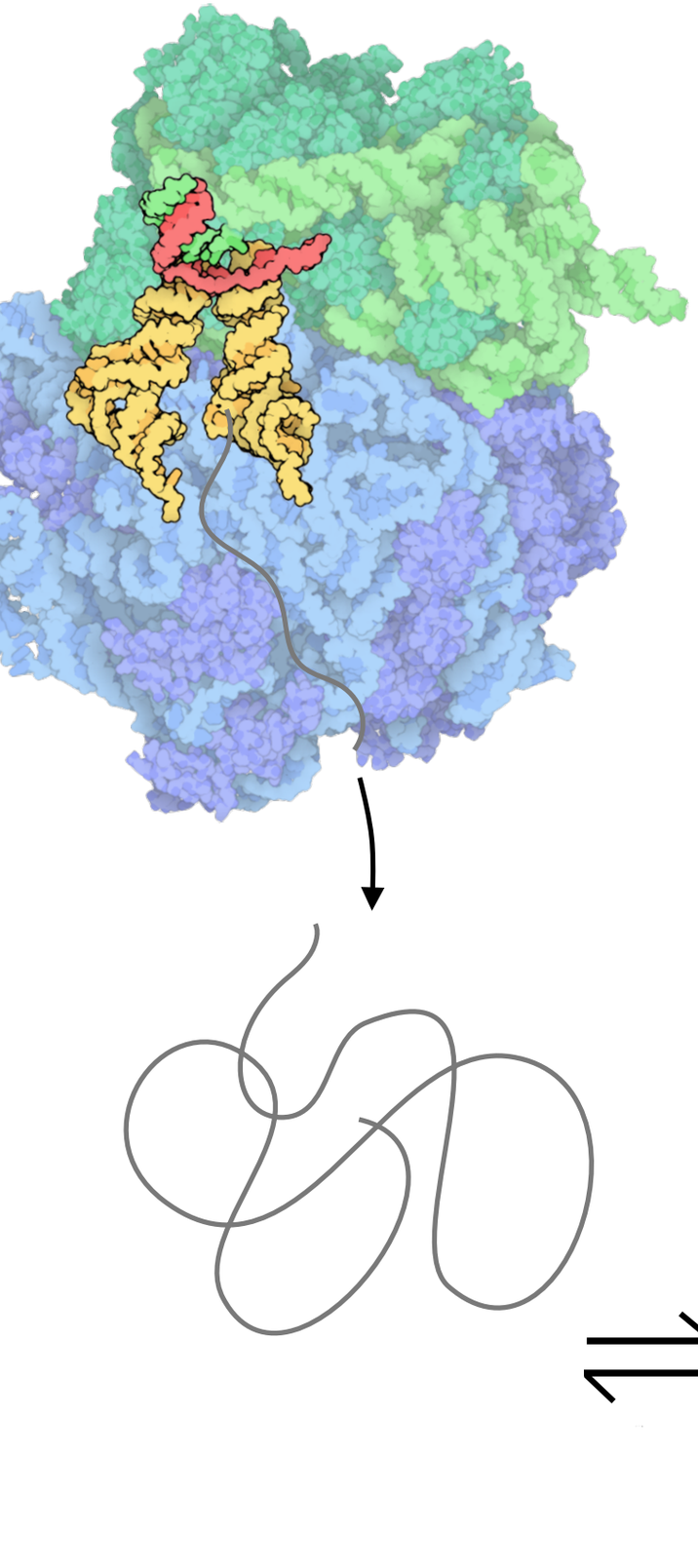

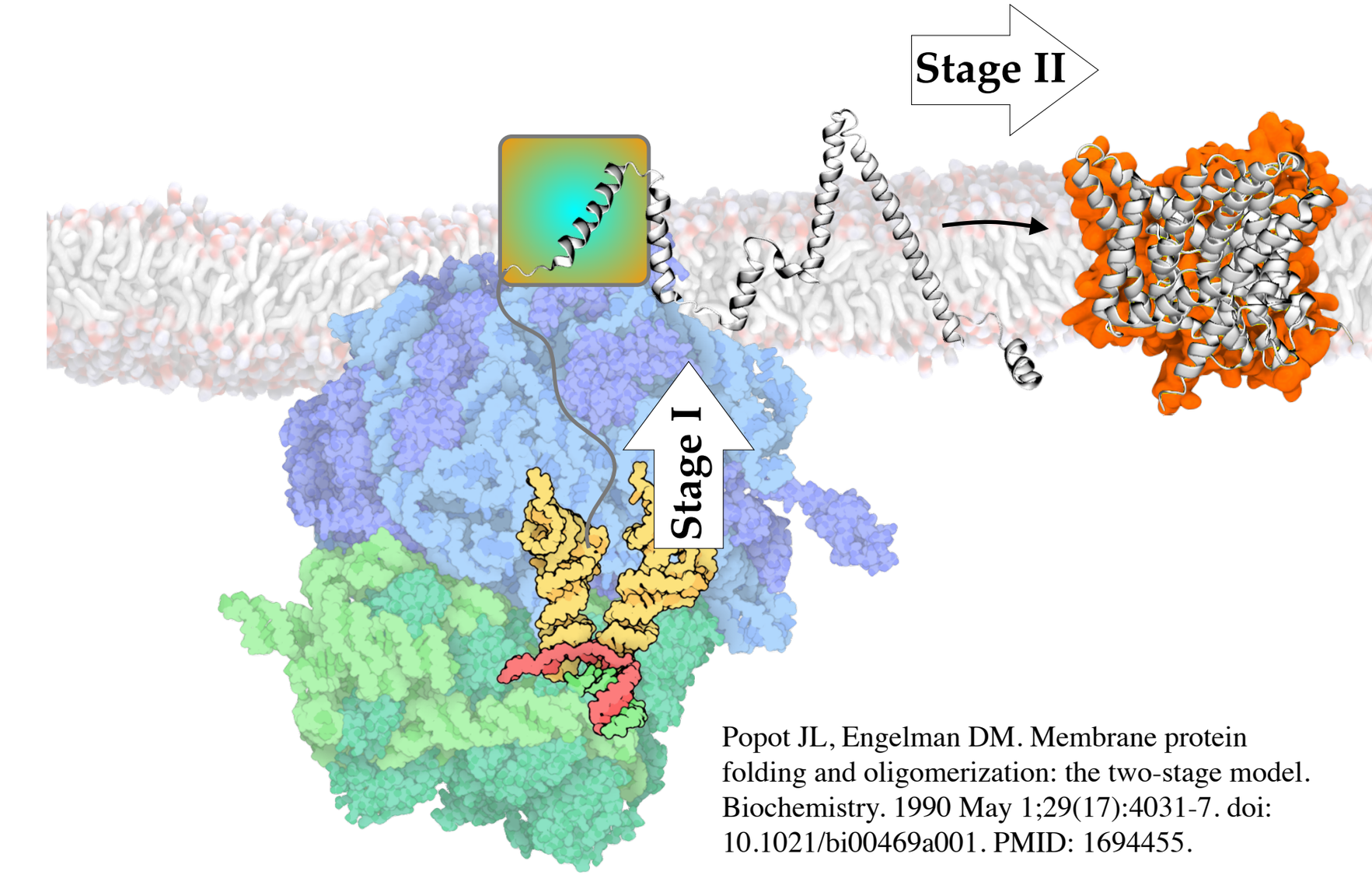

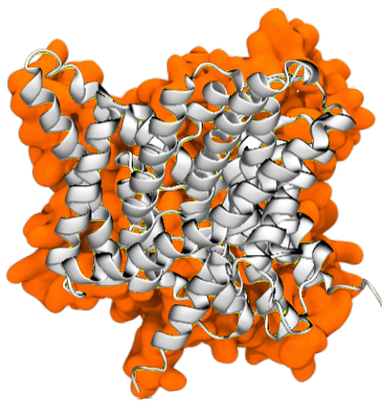

Popot JL, Engelman DM. Membrane protein folding and oligomerization: the two-stage model. Biochemistry. 1990 May 1;29(17):4031-7. doi: 10.1021/bi00469a001. PMID: 1694455.

Alpha-helical membrane protein synthesis

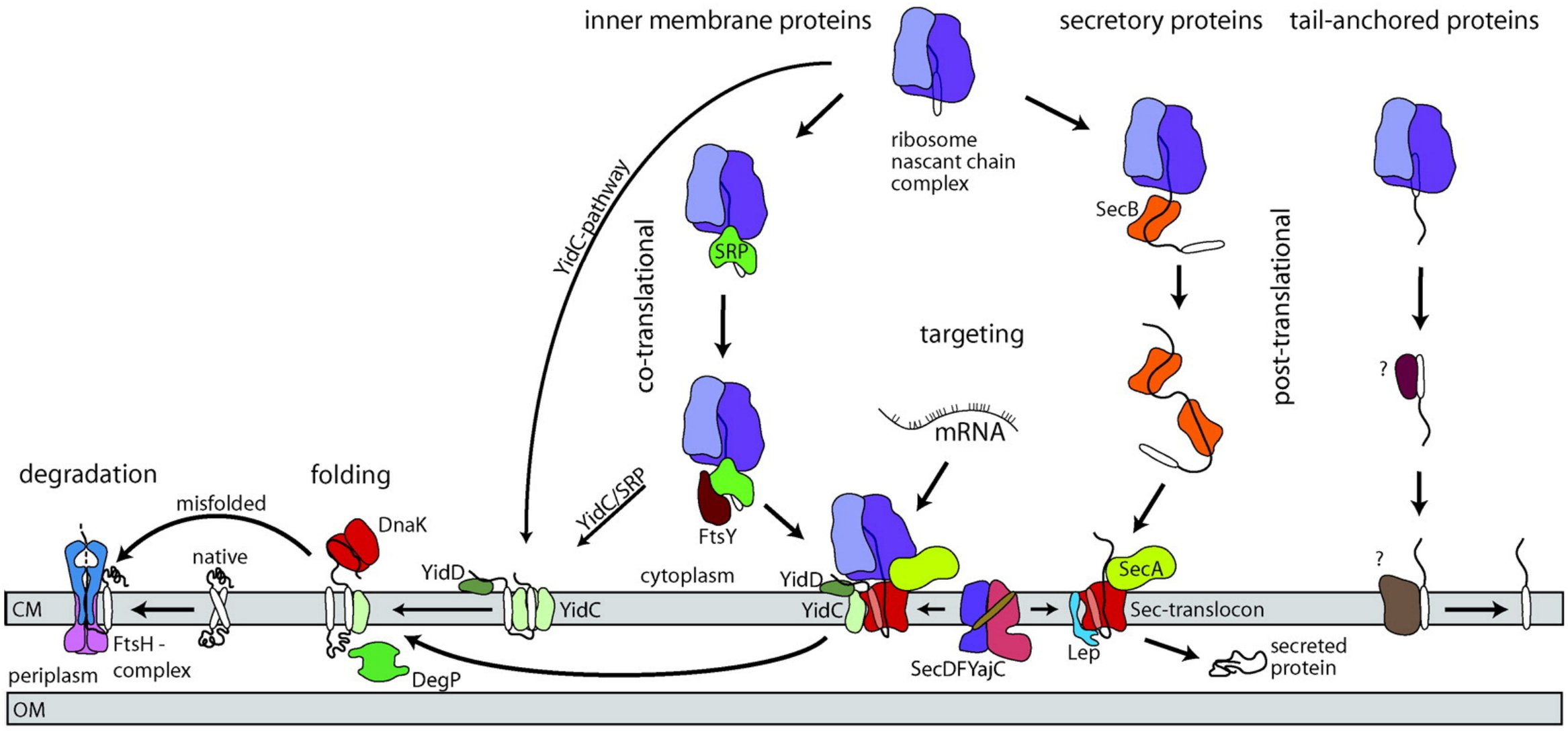

https://doi.org/10.1016/j.bbamcr.2013.10.023

Beta-barrel folding

$\Delta G_{OMPLA(w,l,DL)}$ = -32.5 kcal/mole

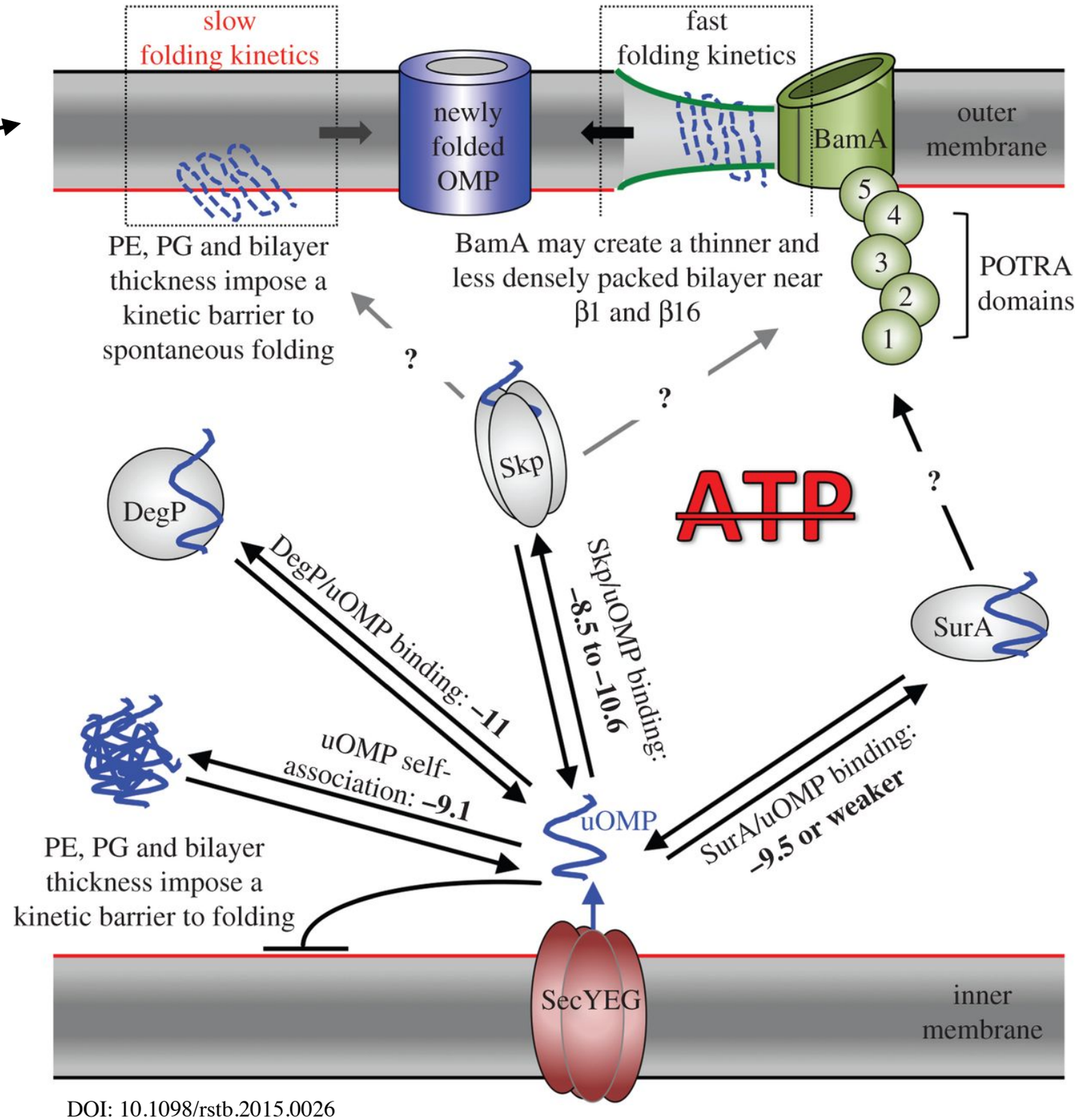

DOI: 10.1098/rstb.2015.0026